The Plant Cell, Vol. 26: 4974–4990, December 2014, www.plantcell.org

The *Arabidopsis* Abiotic Stress-Induced TSPO-Related Protein Reduces Cell-Surface Expression of the Aquaporin PIP2;7 through Protein-Protein Interactions and Autophagic Degradation[C][W][OPEN]

Charles Hachez,[1] Vasko Veljanovski,[1] Hagen Reinhardt,[2] Damien Guillaumot,[3] Celine Vanhee,[4] François Chaumont, and Henri Batoko[5]

Institut des Sciences de la Vie, Université Catholique de Louvain, 1348 Louvain-la-Neuve, Belgium

ORCID ID: 0000-0002-8256-519X (H.B.)

The *Arabidopsis thaliana* multi-stress regulator TSPO is transiently induced by abiotic stresses. The final destination of this polytopic membrane protein is the Golgi apparatus, where its accumulation is strictly regulated, and TSPO is downregulated through a selective autophagic pathway. TSPO-related proteins regulate the physiology of the cell by generating functional protein complexes. A split-ubiquitin screen for potential TSPO interacting partners uncovered a plasma membrane aquaporin, PIP2;7. Pull-down assays and fluorescence imaging approaches revealed that TSPO physically interacts with PIP2;7 at the endoplasmic reticulum and Golgi membranes in planta. Intriguingly, constitutive expression of fluorescently tagged PIP2;7 in TSPO-overexpressing transgenic lines resulted in patchy distribution of the fluorescence, reminiscent of the pattern of constitutively expressed yellow fluorescent protein-TSPO in *Arabidopsis*. Mutational stabilization of TSPO or pharmacological inhibition of the autophagic pathway affected concomitantly the detected levels of PIP2;7, suggesting that the complex containing both proteins is degraded through the autophagic pathway. Coexpression of TSPO and PIP2;7 resulted in decreased levels of PIP2;7 in the plasma membrane and abolished the membrane water permeability mediated by transgenic PIP2;7. Taken together, these data support a physiological role for TSPO in regulating the cell-surface expression of PIP2;7 during abiotic stress conditions through protein-protein interaction and demonstrate an aquaporin regulatory mechanism involving TSPO.

INTRODUCTION

Environmental stresses such as drought, salinity, or cold are common limiting factors for plant growth and development. These stresses impose osmotic and oxidative stresses at the cellular level, and a critical function of the phytohormone abscisic acid (ABA) is to mediate the plant response to these insults during vegetative growth (Finkelstein et al., 2002; Nambara and Marion-Poll, 2005; Yamaguchi-Shinozaki and Shinozaki, 2006). The increase in active ABA levels in plant cells during water-related stress regulates the expression of ABA-responsive genes by interacting with cytosolic and/or organelle-bound receptors and downstream effectors modulating the activity of defined transcriptional regulators (Fujii and Zhu, 2009; Ma et al., 2009; Park et al., 2009; Wu et al., 2009; Shang et al., 2010). It is thought that up to 10% of the *Arabidopsis thaliana* transcriptome is responsive to ABA signaling (Wang et al., 2011). Extensive studies of stress and ABA-induced gene expression during vegetative growth revealed two waves of response: an early transient response peaking at ~3 h and a late sustained response from 10 h onward (reviewed in Finkelstein, 2013). Characteristically, the so-called "early" genes encode regulatory proteins, such as transcription factors, protein kinases, and phosphatases, and a set of proteins of unknown function (Yamaguchi-Shinozaki and Shinozaki, 2006; Fujita et al., 2006). The "late" genes are presumed to contribute to plant adaptation to the stress and encode proteins such as the late embryonic abundant proteins, chaperonins, enzymes, ion and water-channel proteins, and reactive oxygen species scavengers (Fujita et al., 2006; Yamaguchi-Shinozaki and Shinozaki, 2006).

The *Arabidopsis* tryptophan-rich sensory protein/translocator (TSPO) is a multi-stress regulator that is transiently induced in the plant cell (Kreps et al., 2002; Seki et al., 2002; Zimmermann et al., 2004; Winter et al., 2007; Guillaumot et al., 2009; Hermans et al., 2010; Vanhee et al., 2011b). Transcriptionally, ABA-induced TSPO expression peaks at ~3 h postinduction; also, it is one of the most strongly induced "early" genes and is of unknown function. This polytopic membrane protein is encoded by a single locus (At2g47770) in *Arabidopsis* and belongs to the so-called tryptophan-rich sensory protein/peripheral-type benzodiazepine

[1] These authors contributed equally to this work.
[2] Current address: Max-Planck-Institute for Plant Breeding Research, Carl-von-Linné-Weg 10, 50829 Cologne, Germany.
[3] Current address: INRA URGV, 2, Rue Gaston Crémieux, 91057 Evry, France.
[4] Current address: Scientific Institute of Public Health, Rue Juliette Wytsmanstraat 14, 1050 Brussels, Belgium.
[5] Address correspondence to henri.batoko@uclouvain.be.
The author responsible for distribution of materials integral to the findings presented in this article in accordance with the policy described in the Instructions for Authors (www.plantcell.org) is: Henri Batoko (henri.batoko@uclouvain.be).
[C] Some figures in this article are displayed in color online but in black and white in the print edition.
[W] Online version contains Web-only data.
[OPEN] Articles can be viewed online without a subscription.
www.plantcell.org/cgi/doi/10.1105/tpc.114.134080

receptor (TspO/MBR) group of proteins (Papadopoulos et al., 2006). Members of this group of membrane proteins are found, with few exceptions, in organisms ranging from Archaea to metazoans (reviewed in Gavish et al., 1999; Lacapère and Papadopoulos, 2003; Papadopoulos et al., 2006). Since their identification in the late 1970s (Braestrup et al., 1977), TSPOs have been the subject of intensive research, almost exclusively in animal cells, to pinpoint their function. The mammalian 18-kD translocator protein TSPO1 was thought to be encoded by an essential gene and involved in a range of physiological functions and pathologies (Papadopoulos et al., 2006; Rupprecht et al., 2009). A second isoform, TSPO2, is cell specific and functions in erythroid development (Fan et al., 2009). One of the main functions attributed to mammalian TSPOs is their possible involvement in steroid metabolism and mitochondrial physiology (reviewed in Rupprecht et al., 2010), although recent evidence has challenged these acceptations, showing, for example, that mice TSPO1 is not essential and plays no role in steroidogenesis (Morohaku et al., 2014; Sileikyte et al., 2014; Stocco, 2014). It is well documented that TSPOs can form functional homo-oligomers and hetero-oligomers with soluble and membrane-bound partners (reviewed in Papadopoulos et al., 2006). In addition, mammalian TSPOs can regulate the expression or stability of their interacting partner. For instance, overexpression of TSPO1 inhibits the expression of the mitochondrial voltage-dependent anion channel 1 (VDAC1), and the silencing of TSPO1 increases VDAC1 expression in endothelial cells (Joo et al., 2012). Mammalian TSPO can also regulate the expression of a non-interacting protein. For example, TSPO1 is upregulated in $CD4^+$ T cells infected by the human immunodeficient virus 1 (HIV1) and inhibits virus envelope protein expression by promoting its degradation through the endoplasmic reticulum-associated degradation pathway (Zhou et al., 2014).

TSPOs were only recently described in plants (Corsi et al., 2004; Lindemann et al., 2004; Frank et al., 2007; Guillaumot et al., 2009), and in contrast to the situation in mammals, plant TSPOs appear to be nonessential, suggesting a potential functional divergence through the evolution of these proteins. *Arabidopsis* TSPO is transcriptionally regulated by the master bZIP-type transcription factors ABSCISIC ACID-RESPONSIVE ELEMENT BINDING PROTEIN1 (AREB1), AREB2, and ABSCISIC ACID-RESPONSIVE ELEMENT BINDING FACTOR3, which are involved in ABA-responsive element-dependent ABA signaling (Yoshida et al., 2010). TSPO transcripts are detected in desiccation-resistant plant structures and to some extent in senescing leaves but are rapidly and transiently induced in vegetative tissues by ABA and abiotic stresses, including osmotic and salt stress, magnesium deficiency, and high light conditions (Kreps et al., 2002; Seki et al., 2002; Zimmermann et al., 2004; Winter et al., 2007; Guillaumot et al., 2009; Hermans et al., 2010). Accordingly, the protein is readily detected in seeds but not in vegetative tissues under normal growth conditions (Guillaumot et al., 2009). We showed recently that the level of TSPO in the cell is tightly regulated (Guillaumot et al., 2009; Vanhee et al., 2011a, 2011b). TSPO is degraded through a selective autophagic pathway, and targeting of the protein to this pathway requires heme and the ubiquitin-like autophagy-related 8 (ATG8) binding (Vanhee et al., 2011b). Overexpression of TSPO can be detrimental to the cell. In particular, plants and cells overexpressing TSPO are more sensitive to salinity but more tolerant to osmotic stress (Guillaumot et al., 2009).

Water-related stresses ultimately inhibit the growth of both the root and the aerial parts of a plant. Plant cell growth depends mainly on cell elongation driven by water flow and turgidity. The flow of water across cell membranes to regulate growth and transpiration is largely modulated by aquaporins present in the plasma membrane and the tonoplast (Maurel et al., 2008; Chaumont and Tyerman, 2014). The contents and activities of aquaporins are constantly regulated by different factors and at different levels, including transcription, protein stability, subcellular trafficking, and gating (Maurel et al., 2008; Chaumont and Tyerman, 2014). In *Arabidopsis*, the expression of most aquaporins is downregulated during water-related stress, such as drought or salt stress conditions, therefore limiting water loss and potentially creating a hydraulic signal that could induce stomatal closure (Jang et al., 2004; Boursiac et al., 2005; Alexandersson et al., 2010). Although plants express multiple homologous aquaporin isoforms, it is thought that individual aquaporins function nonredundantly (Javot et al., 2003; Postaire et al., 2010; Prado et al., 2013). It is well documented that regulation of aquaporins plays a role in early responses and acclimation to water stress conditions (Chaumont and Tyerman, 2014). However, the mechanisms behind plant aquaporin degradation and/or stability are not fully understood.

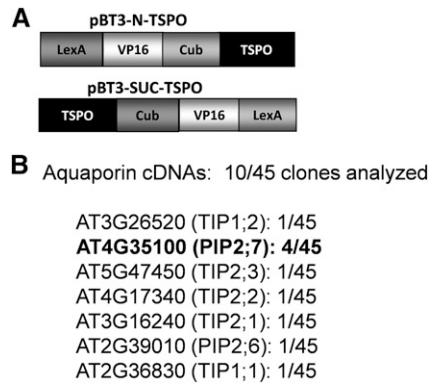

Figure 1. A Split Ubiquitin Screen Identified the *Arabidopsis* PIP2;7 Aquaporin as a Potential TSPO Interacting Partner.

(A) Scheme of the genetic constructs used as bait. In plasmid pBT3-N-AtTSPO, the cDNA encoding TSPO was cloned downstream of the cDNA encoding the chimeric transcription factor LexA-VP16 fused to a C-terminal fragment of ubiquitin (Cub). In plasmid pBT3-SUC-AtTSPO, the cDNA of TSPO was cloned upstream of the cDNA encoding the LexA-VP16-Cub fusion. Each of the bait constructs (pBT3-N-AtTSPO and pBT3-SUC-AtTSPO) was used to screen an *Arabidopsis* cDNA library (complexity of 1.7×10^7) amplified in *Saccharomyces cerevisiae*.
(B) Forty-five yeast clones (35 out of 192 expressing pBT3-N-AtTSPO and 10 out of 43 expressing pBT3-SUC-AtTSPO) displaying the highest β-galactosidase activity (a positive test for bait-dependent interaction; Supplemental Figure 1) were analyzed further by sequencing of the corresponding plasmids, and 10 contained full-length cDNA encoding the listed aquaporin proteins, with 4 out of the 10 encoding PIP2;7.

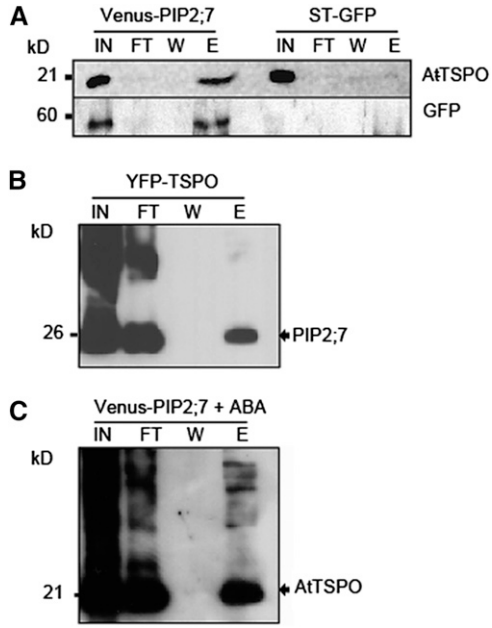

Figure 2. Copurification of PIP2;7 and TSPO from Plant Extracts.

(A) Protein extracts from transgenic *Arabidopsis* dry seeds expressing Venus-PIP2;7 or ST-GFP (negative control) were affinity purified using GFP-Trap. The input (IN), the flow-through (FT), the last wash (W, wash #5), and eluted fractions (E) were analyzed by immunoblotting for TSPO or GFP. TSPO was detected in the eluted fraction (E) from Venus-PIP2;7 expressing extract. See Supplemental Figure 4A for control analysis.
(B) Protein extracts were prepared from transgenic *Arabidopsis* seedlings overexpressing YFP-TSPO and the fusion protein was affinity-purified using GFP-Trap. The various fractions as in **(A)** were analyzed by immunoblotting for PIP2;7. As shown in lane E, endogenous PIP2;7 copurified with YFP-TSPO. See Supplemental Figure 4B for control analysis.
(C) Reverse interaction experiment as shown in **(B)** was tested by incubating transgenic *Arabidopsis* seedlings overexpressing Venus-PIP2;7 in 50 μM ABA for 24 h in order to induce TSPO. Protein extracts after induction were treated as in **(B)** and the various fractions were analyzed by immunoblotting for TSPO. As shown in lane E, the ABA-induced TSPO copurified with Venus-PIP2;7.

In this work, we report the unexpected finding that TSPO interacts intracellularly with the plasma membrane aquaporin PIP2;7 (PLASMA MEMBRANE INTRINSIC PROTEIN 2;7) and downregulates its abundance in the cell. This TSPO-dependent regulation may contribute in reducing the amount of PIP2;7 in the plasma membrane, thus limiting PIP2;7-dependent water transport activity at the plasma membrane under abiotic stress conditions.

RESULTS

The *Arabidopsis* Plasma Membrane Aquaporin PIP2;7 Interacts with TSPO

TSPO-related proteins are known to oligomerize and to form functional hetero-complexes with a diverse array of partners in different cell types (Papadopoulos et al., 2006). To investigate whether this may be the case for the *Arabidopsis* TSPO protein, we screened for potential TSPO interactants using a split-ubiquitin assay in yeast. The full-length TSPO was used as bait and cloned either upstream or downstream of the LexA-VP16-Cub cassette (Figure 1A) (Dualsystems Biotech). Each of the bait constructs was used to screen an *Arabidopsis* cDNA library (complexity of 1.7×10^7) (Dualsystems Biotech). Screening of 1.2×10^7 transformants containing the TSPO bait fused to LexA-VP16-Cub at the N or C terminus yielded 192 and 45 bait-dependent interactants, respectively. We selected 35/192 and 10/45 clones showing the highest β-galactosidase activity for further analysis (Supplemental Figures 1A and 1B). Intriguingly, 10 out of the 45 sequenced clones encoded membrane intrinsic proteins as preys, two from the plasma membrane intrinsic protein (PIP) subfamily (PIP2;7 and PIP2;6), and five from the tonoplast intrinsic protein subfamily (TIP) (Figure 1B). All of these PIP and TIP prey clones were recovered from TSPO fused to LexA-VP16-Cub at the N terminus. PIP2;7 appeared more frequently (four independent clones) than any of the other aquaporins within the subset of 45 possible strong TSPO interactants identified. We

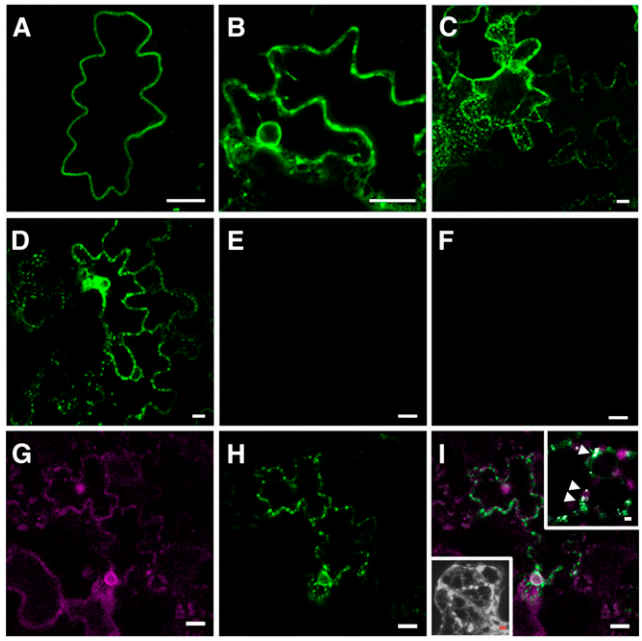

Figure 3. BiFC Demonstrates the PIP2;7-TSPO Interaction in Planta.

(A) to **(F)** Representative confocal images of tobacco epidermal cells transiently expressing YFP-PIP2;7 **(A)**, YFP-TSPO **(B)**, $Venus^N$-PIP2;7 and $Venus^C$-TSPO **(C)**, $Venus^N$-TSPO and $Venus^C$-PIP2;7 **(D)**, $Venus^N$-PIP2;7 **(E)**, and $Venus^C$-TSPO **(F)**.
(G) to **(I)** Coexpression of $Venus^N$-TSPO and $Venus^C$-PIP2;7 (BiFC signal in magenta **[G]**) and ST-GFP (green signal in **[H]**). **(I)** is a merged image of **(G)** and **(H)**. Upper right inset in **(I)** shows colocalization of the BiFC and ST-GFP signals in the Golgi stacks (arrowheads), and lower left inset shows the details of the subcellular distribution of the BiFC signal in the ER and Golgi stacks.
Bars = 20 μm in **(A)** to **(I)** and 2 μm for the insets in **(I)**.

chose therefore to investigate further the possibility that PIP2;7 and TSPO may interact in vivo.

If PIP2;7 and TSPO do interact in vivo in the plant cell and the interaction is strong enough, we reasoned that it may be possible to copurify both proteins. To test this hypothesis, we tagged PIP2;7 at its N terminus with the VenusYFP (yellow fluorescent protein) (Nagai et al., 2002) and constitutively expressed (under the control of the cauliflower mosaic virus p35S promoter) this fusion protein in *Arabidopsis* (Hachez et al., 2014). Tagging PIP proteins at their N terminus with a fluorescent protein does not affect their activity (Fetter et al., 2004; see also below). We reasoned that if Venus-PIP2;7 does interact with the endogenous TSPO, affinity purification of Venus-PIP2;7 could pull down TSPO. We used GFP-Trap (Chromotek) to purify Venus-PIP2;7 from total proteins extracted from T2 transgenic dry seeds enriched in TSPO (Guillaumot et al., 2009) (Supplemental Figures 2 and 3) and checked for the presence of TSPO in the eluted fraction. As a control, we used transgenic *Arabidopsis* seeds overexpressing the membrane-bound Golgi marker protein sialyl transferase fused to green fluorescent protein (ST-GFP), which was shown previously to colocalize with TSPO in the plant cell (Guillaumot et al., 2009). Figure 2A shows protein gel blotting of the different fractions from the pull-down assay. Both Venus-PIP2;7 (lane E, anti-GFP) and the endogenous TSPO (lane E, anti-TSPO) were detected in the eluted Venus-PIP2;7 fraction. The control fraction of the eluted ST-GFP did not contain TSPO (ST-GFP, lane E). We checked that the pull-down of TSPO was PIP2;7 dependent and that as a control, ST-GFP did not copurify with either PIP2;7 or TSPO (Supplemental Figure 4A). Next, we investigated whether this interaction was also active in vegetative tissues. We extracted total proteins from *Arabidopsis* seedlings overexpressing YFP-TSPO (Guillaumot et al., 2009; Vanhee et al., 2011b) and affinity-purified the fusion protein using a GFP-Trap slurry. We found that the endogenous PIP2;7 copurified with YFP-TSPO as shown in Figure 2B (lane E, arrowhead). We showed that YFP-TSPO, as expected, was also present in the eluted fraction (Supplemental Figure 4B). To test the reverse situation, and because TSPO expression is almost undetectable in vegetative tissues (Guillaumot et al., 2009; Vanhee et al., 2011b), we incubated *Arabidopsis* seedlings overexpressing Venus-PIP2;7 in 50 μM ABA for 24 h to induce TSPO (Guillaumot et al., 2009; Vanhee et al., 2011b). As shown in Figure 2C (lane E), protein gel blot analyses showed that the induced TSPO coeluted with the affinity-purified Venus-PIP2;7. These results demonstrate that, when coexpressed, PIP2;7 and TSPO do physically interact in the plant cell.

PIP2;7 and TSPO Interact in the Endoplasmic Reticulum and Golgi

The final destination of PIP2;7 in plant cells is the plasma membrane, while TSPO localizes in the Golgi and to some extent in the endoplasmic reticulum (ER) (Guillaumot et al., 2009; Vanhee et al., 2011a, 2011b). To assess where the two proteins may interact at the subcellular level, we took advantage of the bimolecular fluorescence

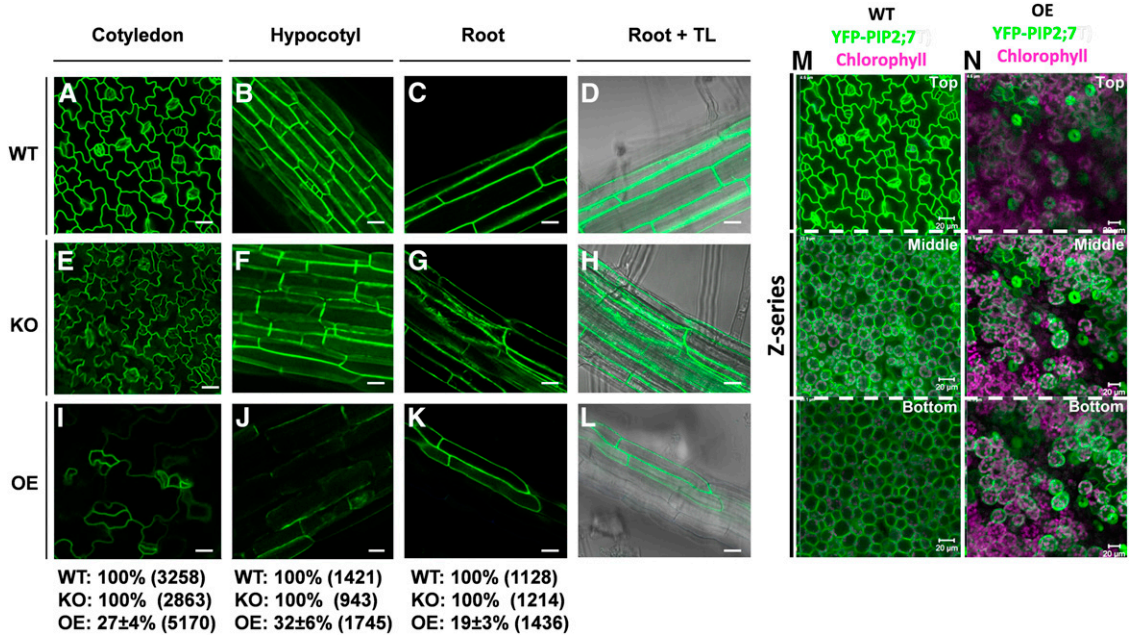

Figure 4. Overexpression of TSPO Differentially Regulates the Expression of Constitutively Expressed YFP-PIP2;7.

Representative confocal images of transgenic *Arabidopsis* seedlings overexpressing YFP-PIP2;7. Images of cotyledons (**[A]**, **[E]**, and **[I]**), hypocotyls (**[B]**, **[F]**, and **[J]**), and roots (**[C]**, **[G]**, and **[K]**) merged with transmitted light images (**[D]**, **[H]**, and **[L]**) from the wild-type background, a knockout line for TSPO (KO), or a transgenic line overexpressing TSPO (OE). The percentage of cells (in parenthesis the total number of cells analyzed) showing detectable YFP-PIP2;7 fluorescence from random samples and acquired images using identical settings are given ± the SE of the mean for each organ. **(M)** and **(N)** show the detection of YFP-PIP2;7 (green channel) and chlorophyll autofluorescence (magenta) from the acquired Z-series (depth of 18.5 μm in **[M]** and 27.7 μm in **[N]**) from the epidermis (top) to the mesophyll cells (bottom) of the wild-type **(M)** or TSPO overexpressing **(N)** cotyledon. Bars = 20 μm.

complementation (BiFC) technique (Bracha-Drori et al., 2004). We prepared genetic constructs encoding chimeric fusions in which both interactants were fused N-terminally to either the N-terminal ($Venus^N$) or the C-terminal half ($Venus^C$) of the split VenusYFP (Besserer et al., 2012). These chimeric constructs driven by a p35S promoter were transiently expressed in tobacco (*Nicotiana tabacum*) leaf epidermal cells, and the reconstitution of Venus was assessed by confocal microscopy imaging. We also expressed PIP2,7 and TSPO N-terminally tagged with the full-length Venus. To ascertain the organelles highlighted by the BiFC signal, we coexpressed the tested combinations with ST-GFP, which was previously shown to colocalize with TSPO in the plant cell (Guillaumot et al., 2009). Figures 3A and 3B show examples of imaged cells highlighting the subcellular localization of Venus-PIP2;7 and YFP-TSPO. As expected, Venus-PIP2;7 fluorescence outlined the cell, consistent with the localization described so far for all tested PIP2 isoforms in the plasma membrane (i.e., Boursiac et al., 2005; Besserer et al., 2012). Coexpression of $Venus^N$-PIP2;7 and $Venus^C$- TSPO (Figure 3C) or $Venus^N$-TSPO and $Venus^C$-PIP2;7 (Figure 3D) generated a reconstituted Venus signal, confirming the in vivo interaction of TSPO and PIP2;7. $Venus^N$-PIP2;7 (Figure 3E) or $Venus^C$-TSPO (Figure 3F) when expressed alone did not generate any fluorescence, and the same was true for the other split variants expressed alone. When the spliced-Venus complementary couples containing TSPO and PIP2;7 were coexpressed with ST-GFP (Figures 3G to 3I), the resulting BiFC signal and ST-GFP signal colocalized in the ER and Golgi stacks (Figure 3I, upper right inset, arrowheads). The BiFC signal was found both in the Golgi stacks and the ER network (Figure 3I, bottom left inset). In accordance with the results from the pull-down assay, the BiFC data confirm that PIP2;7 and TSPO do interact in the plant cell and most likely within the ER and Golgi membranes.

Constitutively Expressed TSPO Downregulates Overexpressed PIP2;7

The transcripts of PIP2;7 and TSPO appear to be developmentally regulated and almost mutually exclusive during seed development (Supplemental Figure 2). We wondered whether this may also be the case at the protein level. Knowing that TSPO is enriched in dry *Arabidopsis* seeds, we analyzed by protein gel blot the dynamics of the PIP2;7 and TSPO levels in germinating seeds and up to 4 d postimbibition (Supplemental Figure 3). The level of TSPO rapidly declined in wild-type germinating seeds and became undetectable after 2 d of imbibition, consistent with the evolution of transcript levels (Zimmermann et al., 2004; Winter et al., 2007). In contrast, we detected a paralleled steady increase of PIP2;7 with time (Supplemental Figure 3A). A similar pattern was observed in a TSPO knockout line (SALK_066561C; Supplemental Figure 3B), suggesting that the developmental regulation of PIP2;7 at the protein level during germination may not be linked per se to the presence of TSPO. TSPO is only transiently expressed in *Arabidopsis* vegetative tissues during exposure to abiotic stress conditions (Guillaumot et al., 2009). To investigate whether the expression of TSPO may have any posttranslational consequences upon PIP2;7, we overexpressed (p35S promoter) Venus-PIP2;7 in transgenic homozygous *Arabidopsis* lines constitutively (p35S promoter) expressing TSPO. For comparison, we also transformed Venus-PIP2;7 in wild-type *Arabidopsis* and in a TSPO knockout (SALK_066561 C) line. Representative confocal images in Figure 4 show that the detection of Venus-PIP2;7 fluorescence within different organs was drastically affected by the constitutive expression of TSPO. In the wild-type and knockout (KO) backgrounds, Venus-PIP2;7 fluorescence was detected in every cell of the cotyledon, the hypocotyl, and the root, accessible to confocal imaging (Figures 4A to 4D and 4E to 4H). Intriguingly, we consistently found that in every organ of the primary transgenic lines examined, when detected, the Venus-PIP2;7 signal intensity varied from cell to cell in the TSPO (OE) background and was completely undetectable in 70 to 80% of the cell types analyzed (Figures 4I to 4L). This observation was consistent in two independent homozygous transgenic lines (OE8 and OE9; Vanhee et al., 2011b) constitutively expressing TSPO. This unexpected pattern of Venus-PIP2;7 fluorescence distribution in the TSPO OE background cannot be explained by a possible positional effect, since all of the generated transgenic lines in these backgrounds driven by a constitutive p35S promoter showed the same patchy fluorescence, but this patchy fluorescence was not observed in the wild-type or KO backgrounds. In addition, from segregating T2 transgenic plants after selfing, we could recover hygromycin-sensitive plants showing the wild-type pattern of Venus-PIP2;7 (Supplemental Figure 5), suggesting that these individuals were indeed devoid of the TSPO transgene and that

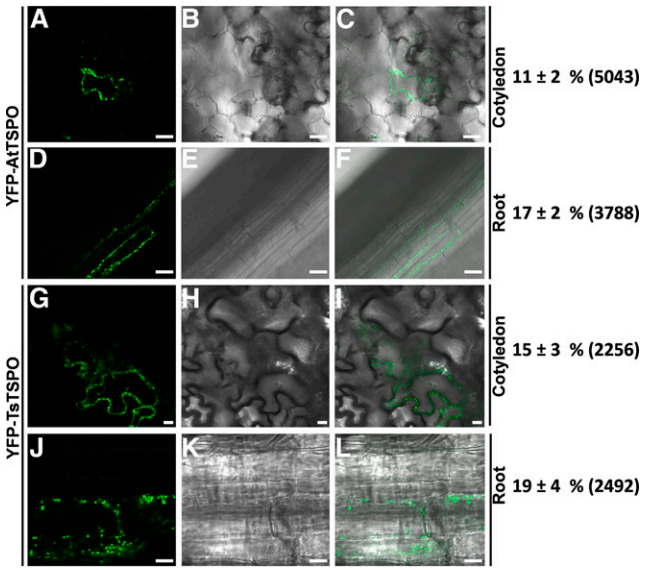

Figure 5. Differential Expression of Fluorescent Protein-Tagged TSPO from *A. thaliana* or *E. salsugineum* Overexpressed in *Arabidopsis*.

Representative confocal images of cotyledon expressing *Arabidopsis* YFP-At-TSPO (**[A]** green channel, **[B]** transmitted light, and **[C]** merge) and *E. salsugineum* (formerly *T. salsuginea*) YFP-Ts-TSPO (**[G]** green channel, **[H]** transmitted light, and **[I]** merge), root expressing YFP-At-TSPO (**[D]** green channel, **[E]** transmitted light, and **[F]** merge) and YFP-TsTSPO (**[J]** green channel, **[K]** transmitted light, and **[L]** merge). The percentage of cells (total number of cells analyzed in parenthesis) showing detectable YFP fluorescence from random samples and acquired images using identical settings are given ± the SE of the mean for each organ. Bars = 20 μm in **(A)** to **(F)** and 10 μm in **(G)** to **(L)**.

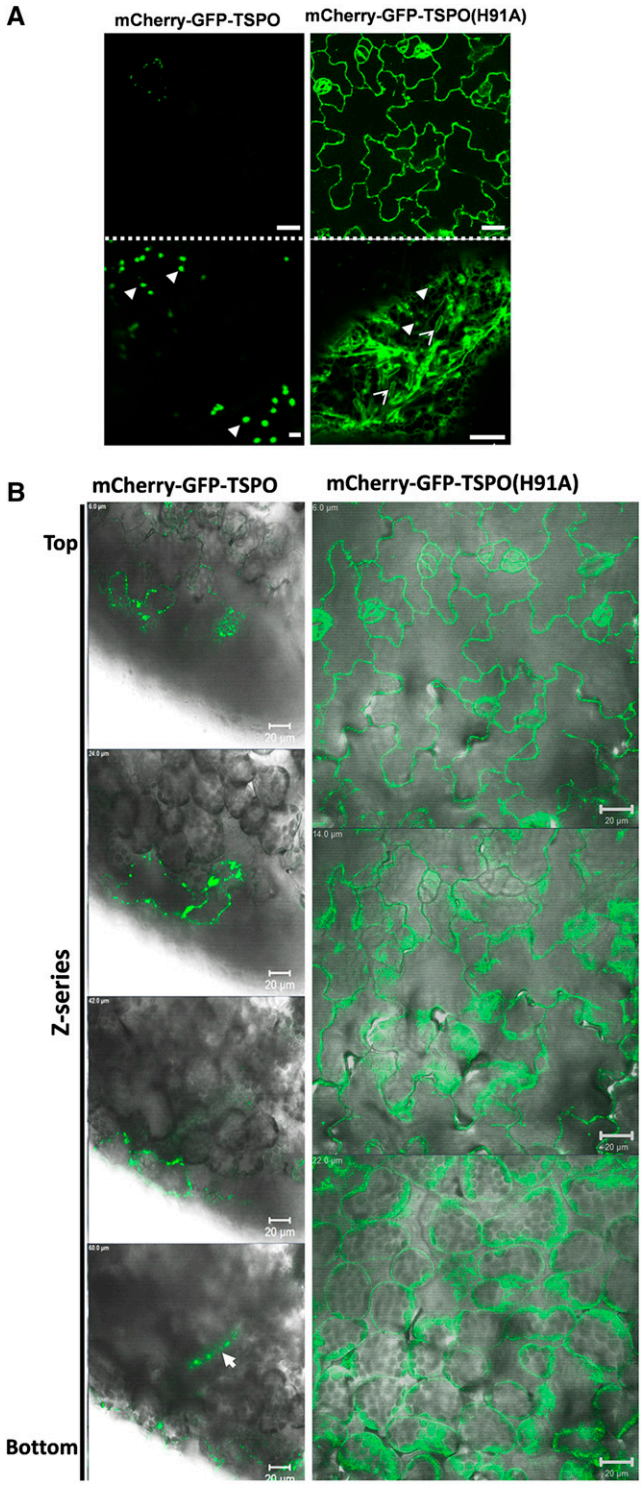

Figure 6. A Defined Point Mutation in TSPO Stabilizes the Overexpressed Protein in Transgenic *Arabidopsis*.

The wild-type TSPO and the mutant form harboring the H91A substitution were tagged with both the monomeric Cherry variant of the red fluorescent protein and GFP, and the resulting fusion was constitutively expressed in transgenic *Arabidopsis*.

overexpressed TSPO was responsible for the patchy distribution of Venus-PIP2;7 fluorescence. As shown in Figure 4, the patchy distribution of Venus-PIP2;7 fluorescence was not restricted to the epidermal cell layer of, for instance, the cotyledon but was also evident in the mesophyll cells (Figures 4M and 4N, compare the Venus-PIP2;7 signal in the Z-stack optical sections from the wild type and OE). Since Venus-PIP2;7 is constitutively expressed, these results suggest that coexpression of TSPO may downregulate Venus-PIP2;7 in a cell-dependent manner. To further investigate this possibility, we first examined the stability of the overexpressed fluorescent protein-tagged TSPO in transgenic *Arabidopsis* plants.

Fluorescence of Overexpressed YFP-TSPO Is Restricted to Some *Arabidopsis* Cells

We showed previously that TSPO is only transiently expressed in the plant cell and induced by abiotic stresses and that constitutively expressed TSPO can be detrimental to cultured plant cells (Guillaumot et al., 2009). The presence of TSPO in cells appears to be tightly regulated, and when required, the protein is efficiently downregulated through a selective autophagic pathway (Vanhee et al., 2011b). We generated homozygous *Arabidopsis* transgenic lines overexpressing YFP-TSPO. Confocal imaging analysis of these lines, irrespective of the relative strength of the constitutive promoter and the backbone of the binary vector used (single or double p35S in pCambia or enhanced p35S in pVKH-En6; Batoko et al., 2000; Saint-Jore et al., 2002), resulted in a patchy distribution of the YFP-TSPO fluorescence (Figures 5A to 5F). This differential stability of the constitutively expressed TSPO protein fusion was not a peculiarity of the *Arabidopsis* protein, since the *Thellungiella salsuginea* (a stress-tolerant, close relative of *Arabidopsis* that was recently renamed *Eutrema salsugineum*) TSPO-related protein (Ts-TSPO), when overexpressed in *Arabidopsis*, showed the same patchy distribution (Figures 5G to 5L). The fluorescence generated by the protein fusions containing either of the two plant TSPOs could be detected, with variable intensity, in <20% of the imaged cells, irrespective of the sampled organ (Figure 5).

We showed previously that downregulation of TSPO in the plant cell requires heme binding (Vanhee et al., 2011b). Substitution of the histidine residue at position 91 to alanine in TSPO (H91A), a histidine residue thought to be required for heme iron axial coordination, resulted in a substantial reduction of heme binding in vitro and reduced degradation in vivo (Vanhee et al., 2011b). Downregulation of TSPO requires H91 in addition to an active autophagic pathway. We reasoned that if this patchy

(A) Representative confocal images comparing GFP fluorescence in a large field of view (upper panels) and the subcellular distribution of the signal (lower panels). The closed arrowheads in the bottom panels point to Golgi stacks, and the open arrowheads in the bottom right panel point to ER bodies. Bars = 20 μm in upper panels, 2 μm in bottom left, and 10 μm in bottom right.
(B) Z-stack series (54-μm depth) of GFP (green channel) imaging from the epidermis (top) to the mesophyll (bottom) cells and merged with transmitted light (gray channel), showing the detection of GFP signal in different cell layers of a cotyledon (limited to a few cells mainly in the epidermis in the case of the wild-type protein). The arrow points to GFP fluorescence along a vein. Bars = 20 μm.

distribution of the fluorescence generated by the TSPO-containing fusions is due to the active downregulation of the expressed chimera, then overexpression of the H91A mutant form of TSPO should be more stable and evenly detected in all cell types. To test this hypothesis, we tagged the wild type and the H91A variant of TSPO with both mCherry (monomeric variant of DsRed) and GFP and then overexpressed these constructs in transgenic *Arabidopsis* plants, under the control of the same constitutive promoter (p35S). As shown in Figure 6 and as expected, the wild-type fusion protein showed the same patchy distribution and was mainly targeted to the Golgi stacks in the cotyledon of the transgenic seedling (top and bottom left panels in Figure 6A). In contrast, the H91A fusion was present in every cell and highlighted mainly the ER (top and bottom right panels in Figure 6A). Interestingly, the H91A fusion also outlined ER bodies (bottom right panel in Figure 6A, open arrowheads), a structure not highlighted by the wild-type protein fusion, and was also detected in mobile structures that were most likely Golgi stacks (bottom right panel in Figure 6A, closed arrowheads). As exemplified in Figure 6B, which shows a subset of *z*-stacks from an imaged cotyledon, the wild-type TSPO and the H91A mutant fusions driven by the same constitutive promoter presented a striking difference in their distribution in the various cell types accessible to confocal imaging. While the wild-type TSPO was mostly detected in some epidermal cells, consistent with previous observations, the H91A variant was detected in every cell, suggesting that the H91A mutant form of TSPO is less prone to downregulation in the cell. This difference in apparent stability between the wild-type and the heme binding-deficient mutant form of TSPO could be linked to the less efficient degradation of the H91A mutant form through the autophagic pathway as compared with the wild-type fusion. These results confirm that efficient regulatory degradation of TSPO requires heme binding; thus, the observed patchy distribution of the fluorescence generated by the wild-type fusion protein may be due to the effective downregulation of the fusion by most cells.

Fluorescence of Tagged PIP2;7 Is Altered in the Presence of TSPO

Next, we checked whether coexpression of TSPO and PIP2;7 had any consequence on the stability of either protein in plant tissues. We reciprocally crossed transgenic *Arabidopsis* lines overexpressing either CFP-PIP2;7 or YFP-TSPO. Representative confocal images of cotyledons expressing CFP-PIP2;7 and/or YFP-TSPO are shown in Figure 7. In the wild-type background (inset in upper panel), CFP-PIP2;7 fluorescence is detected in every cell imaged as shown previously for Venus-PIP2;7 (Figure 4). When crossed with a transgenic line overexpressing YFP-TSPO, the CFP-PIP2;7 signal in the resulting F1 hybrid became patchy (Figure 7, bottom panel, merge) as did the YFP-TSPO signal (Figure 7, middle panel), suggesting that coexpression of YFP-TSPO and CFP-PIP2;7 had a down-regulatory effect upon CFP-PIP2;7 in most cells. As shown in the Venn diagram (Figure 7), ~22% of the cells imaged from F1 plants showed CFP-PIP2;7 fluorescence, 16.5% showed YFP-TSPO fluorescence, and 6% of the cells showed both signals, suggesting that PIP2;7 and TSPO are not necessarily mutually exclusive when coexpressed. Consistent with the observed alteration of the PIP2;7-derived signal in

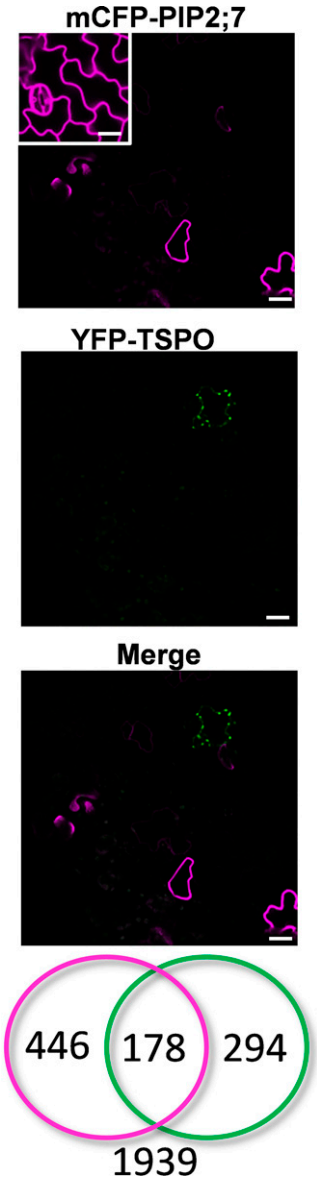

Figure 7. Coexpression of CFP-PIP2;7 and YFP-TSPO Results in Patchy Distribution of Both Fusion Proteins.

Reciprocal crosses between transgenic *Arabidopsis* lines expressing CFP-PIP2;7 or YFP-TSPO were generated and the offspring analyzed for monomeric CFP and YFP fluorescence. The upper panel shows a representative image of CFP expression in cells of a cotyledon compared with the pattern observed in the parental line shown in the inset. The middle panel shows the distribution of YFP expression, and the bottom panel the merged image. The Venn diagram indicates the number of cells with CFP fluorescence (magenta), YFP fluorescence (green), and the number in the intersection indicates cells containing both fluorescent signals. The number of nonfluorescent cells is indicated outside of the circles. Bars = 20 μm.

untagged TSPO-overexpressing lines, these results suggest that both the untagged and the fluorescent fusion forms of TSPO are active in preventing the accumulation of PIP2;7-containing fusion proteins in most plant cells. The strong p35S is known to induce in some cases homology-dependent transcriptional silencing (Mlotshwa et al., 2010), in which case we should observe no expression of the transgenes in all tissues of the silent plant. To exclude the possibility that the patchy cellular phenotype may be due to a potential deleterious effect of the heterologous strong p35S promoter, we expressed RFP-TSPO under the control of the *Arabidopsis* mild constitutive promoter ubiquitin 10 (Grefen et al., 2010). As shown in Supplemental Figure 6, expression of RFP-TSPO was also patchy and when coexpressed with YFP-PIP2;7 (driven by its endogenous promoter), the YFP signal also became patchy. Since TSPO and PIP2;7 interact in vivo, the patchy distribution of these fluorescent chimera may be a consequence of the active degradation of TSPO, targeting the TSPO-PIP2;7 complex for degradation through the autophagic pathway as shown previously for TSPO (Vanhee et al., 2011b).

Inhibition of Autophagy Concomitantly Enhances the Stability of Both TSPO and PIP2;7

We reasoned that if the decreased abundance of PIP2;7 in the presence of TSPO is linked to the active autophagy-dependent degradation of TSPO, stabilizing the latter by transiently inhibiting the autophagic pathway should simultaneously enhance the stability of PIP2;7. To test this hypothesis, we treated *Arabidopsis* seedlings coexpressing CFP-PIP2;7 and YFP-TSPO with the phosphatidylinositol-3-kinase inhibitor 3-methyladenine (Seglen and Gordon, 1982) or with the more potent and specific autophagosome formation inhibitor Spautin 1, which promotes the phosphatidylinositol-3-kinase complex degradation (Liu et al., 2011). After 24 h of incubation with the compounds, protein extracts from the treated and control samples were analyzed by protein gel blotting. As shown in Figure 8A, both inhibitors increased the relative amount of YFP-TSPO detected ~6- to 8-fold compared with the control and increased the amount of CFP-PIP2;7 by ~5-fold. These results suggest that PIP2;7 is likely downregulated, at least in part, by the same pathway as TSPO in the cell. If this is the case, then expression of a stable mutant form of TSPO should have relatively little effect on PIP2;7 downregulation. We expressed a more stable form of TSPO (mutant H91A) and compared the effect of the mutant and wild-type TSPO on the levels of endogenous PIP2;7. We probed extracts from transgenic plants expressing either mCherry-GFP-TSPO or mCherry-GFP-TSPO (H91A) for the endogenous PIP2;7 level. As shown in Figure 8B, the detected endogenous levels of monomeric and dimeric PIP2;7 forms in plants expressing mCherry-GFP-TSPO was at least half the level detected in plants expressing mCherry-GFP-TSPO (H91A). The latter was comparable to the level of endogenous PIP2;7 in the corresponding extracts from untransformed control

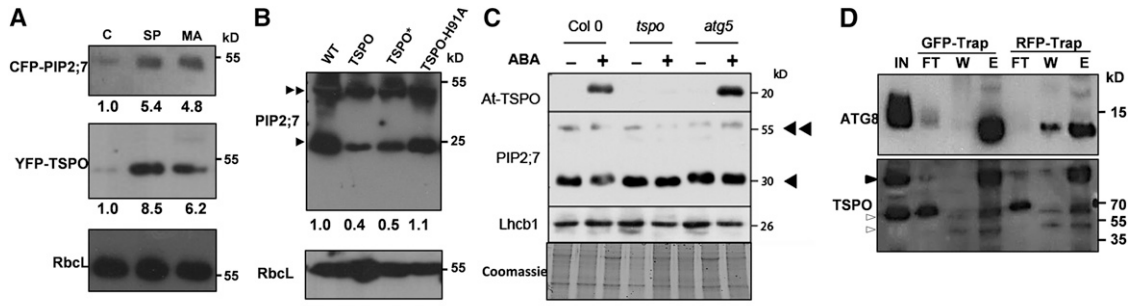

Figure 8. TSPO and PIP2;7 Are Concomitantly Downregulated through the Autophagic Pathway.

(A) *Arabidopsis* transgenic seedlings coexpressing CFP-PIP2;7 and YFP-TSPO were incubated for 24 h in 50 μM Spautin (lane SP) or 5 mM methyladenine (lane MA), and control seedlings (lane C) received DMSO as a mock control. Total proteins were analyzed by immunoblotting and the relative levels of CFP-PIP2;7 and YFP-TSPO quantified, using the Rubisco large subunit (RbcL) as a loading control. Each treatment (signal intensity divided by that of the corresponding RbcL) was compared with the control (ratio C/RbcL normalized to 1).

(B) *Arabidopsis* wild-type (lane WT) and transgenic seedlings overexpressing untagged TSPO (lane TSPO), YFP-TSPO (lane TSPO*), or the H91A substitution mutant (lane TSPO-H91A) tagged with mCherry-GFP were analyzed as in **(A)** but the blot was probed for the endogenous PIP2;7, with RbcL as a loading control. For relative comparisons with the wild type, the PIP2;7 monomer (single arrowhead), and the dimer (double arrowhead), signal intensities were summed and divided by the intensity of the corresponding RbcL signal and the wild type/RbcL ratio was normalized to 1.

(C) ABA-dependent induction of endogenous TSPO can downregulate endogenous PIP2;7. *Arabidopsis* wild-type (lane Col-0), a TDNA insertional knockout mutant for TSPO (lane *tspo*), and Atg5 null mutant deficient in macroautophagy (lane atg5) seedlings were incubated in 50 μM ABA and sampled after 48 h. Total protein extracts were analyzed by protein gel blotting and the levels of endogenous TSPO and PIP2;7 compared with the appropriate mock sample (no ABA). Since RbcL appeared to be sensitive to relatively long ABA incubation periods, we used light-harvesting chlorophyll binding protein (Lhcb1) as loading control, and a Coomassie blue-stained replica of the transferred gel is shown. Double arrowhead indicates PIP2;7 dimers, and the single arrowhead indicates PIP2;7 monomers.

(D) Degradation of TSPO involves interaction with ATG8 in vivo. Microsomal proteins from *Arabidopsis* transgenic seedlings overexpressing mCherry-GFP-TSPO were solubilized and subjected to affinity purification using GFP-trap and RFP-trap slurry, and the input (IN), the flow-through (FT), the last wash (W; wash #5), and the eluted fractions (E) were analyzed by immunoblotting for ATG8 and TSPO. Endogenous ATG8 was copurified (lanes E, upper blot) with mCherry-GFP-TSPO (lower blot). Closed arrowhead, full-length fusion protein; open arrowheads, degradation products.

plants. To exclude any artifacts from overexpression, we investigated whether physiological levels of TSPO could downregulate endogenous PIP2;7 through the autophagic pathway. We induced TSPO in the wild type, the TSPO knockout, and in the autophagy-deficient *atg5* mutant backgrounds. The levels of TSPO and PIP2;7 were assessed by protein gel blotting and compared with mock-treated samples. As shown in Figure 8C, after 48 h of ABA treatment, TSPO induction in the wild type coincided with the downregulation of the level of PIP2;7. The PIP2;7 level was not affected in extracts of TSPO KO plants, and interestingly, although TSPO was also induced in the *atg5* mutant, the level of PIP2;7 remained relatively unchanged after 48 h of ABA treatment, suggesting that the downregulation observed in the wild type requires the autophagic pathway. Mutational analysis suggested that TSPO is degraded through a selective autophagic pathway and that TSPO may interact with the autophagic regulator ATG8 (autophagy-related 8) through an ATG8 interacting motif (Vanhee et al., 2011b). To confirm the downregulation of TSPO through a selective autophagic pathway, we used mCherry-GFP-TSPO and pull-down assays to validate the TSPO

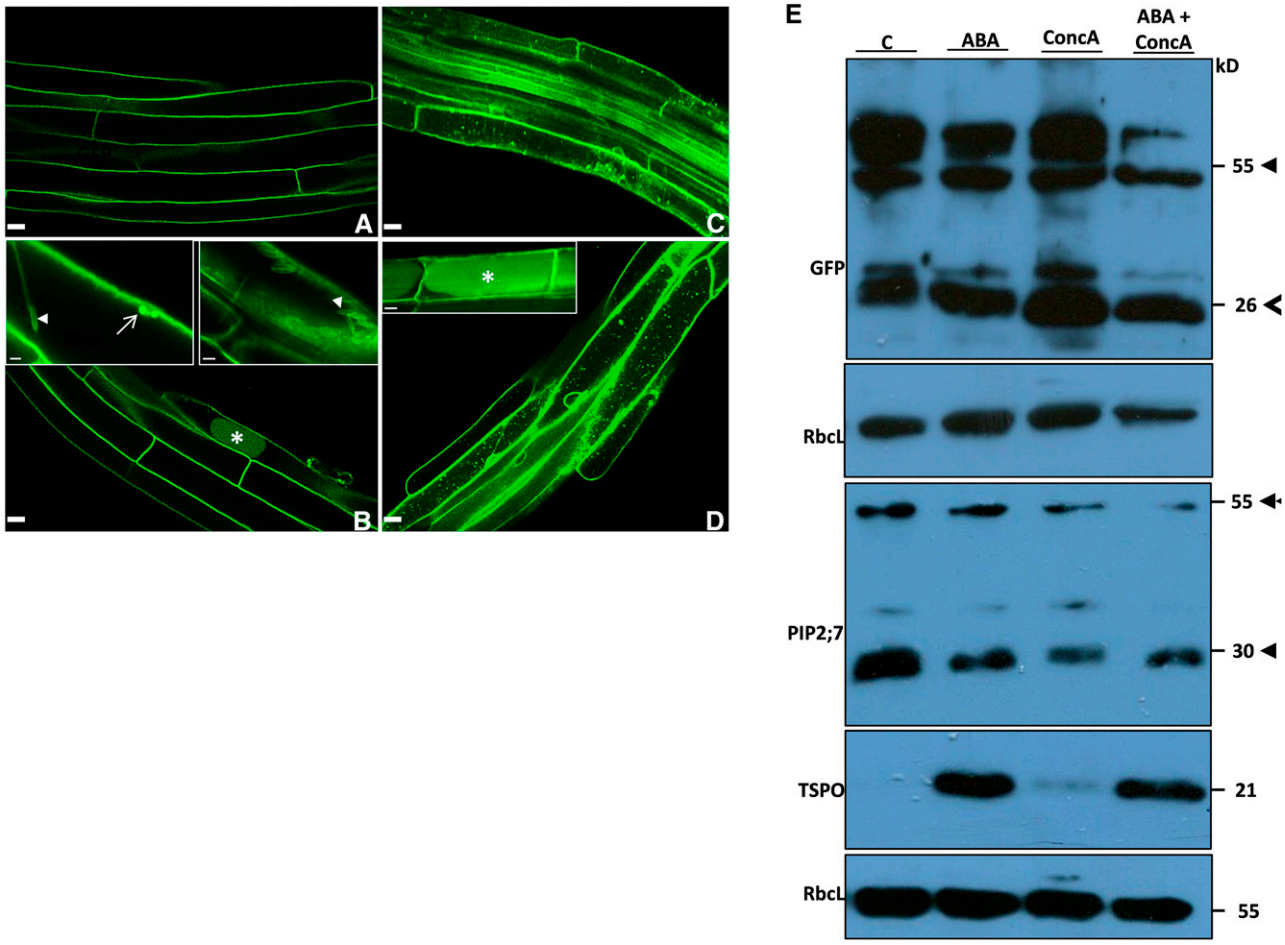

Figure 9. ABA Treatment Enhances YFP-PIP2;7 Degradation through the Vacuole.

Transgenic seedlings expressing YFP-PIP2;7 were incubated for 24 h in ABA (100 μM), ConcA (1 μM), or both. At the end of the incubation period, the seedlings were sampled for confocal imaging (**[A]** to **[D]**) and total protein extractions followed by protein gel blot analyses **(E)**.

(A) Confocal imaging shows YFP fluorescence in the plasma membrane of control root cells.

(B) After ABA treatment, confocal imaging shows some of the YFP fluorescence in the vacuole (*) of root epidermal cells and internally in ER body-like structures (arrowhead in inserts) and in invaginations of the plasma membrane (arrow).

(C) After ConcA treatment, in addition to the plasma membrane, confocal imaging shows YFP fluorescence in intracellular puncta, most likely autophagosomes.

(D) After a combined ABA (100 μM) and ConcA (1 μM) treatment, confocal imaging shows YFP fluorescence in autophagosomes (puncta) and in the vacuole (*) of root cells. Bars = 10 μm in the panels and 5 μm for the insets.

(E) The levels of PIP2;7 were probed by protein gel blotting using anti-PIP2;7 and anti-GFP. PIP2;7 and At-TSPO levels from treated samples were compared to the appropriate mock control. GFP panel: open arrowhead indicates free GFP from YFP-PIP2;7 degradation, and arrowhead indicates full-length YFP-PIP2;7. PIP2;7 panel: double arrowhead indicates endogenous PIP2;7 dimer, and single arrowhead indicates PIP2;7 monomer.

[See online article for color version of this figure.]

interaction with ATG8. Microsomes were prepared from transgenic seedlings overexpressing mCherry-GFP-TSPO. The solubilized microsomal fraction was incubated with a GFP-Trap or RFP-Trap slurry. As shown in Figure 8D, the eluted fractions from GFP-Trap and RFP-Trap copurified ATG8, confirming that TSPO does interact in vivo with ATG8; thus, TSPO is degraded by a selective autophagy mechanism. These results suggest that expression of TSPO can reduce the level of endogenous PIP2;7 in the cell and that the more stable H91A mutant form has almost no effect on this process. We showed previously that overexpression of TSPO in *Arabidopsis* cultured cells resulted in enhanced tolerance to osmotic stress (Guillaumot et al., 2009).

To verify that PIP2;7 is indeed degraded through the autophagic pathway during abiotic stress conditions, we treated YFP-PIP2;7-expressing plants with ABA, Concanamycin A (ConcA), or both for 24 h and analyzed the subcellular distribution of YFP fluorescence by confocal imaging and the levels of TSPO, YFP-PIP2;7, and endogenous PIP2;7 by protein gel blotting. As shown in Figure 9, ABA treatment induced TSPO and the YFP (Venus) signal could be detected in the vacuole of some root epidermal cells in addition to intracellular compartments morphologically resembling ER bodies. ConcA alone could induce detectable levels of TSPO, and this treatment also triggered the accumulation of YFP fluorescence in punctate structures reminiscent of autophagosomes. When the root cells were treated with both ABA and ConcA, YFP fluorescence was found in punctate structures and in the vacuole of most cells. The proliferation of punctate structures in the cytoplasm and possibly in the vacuole may reflect the inhibition of vacuolar hydrolases by ConcA. YFP fluorescence in the vacuolar lumen indicates the degradation of the transmembrane part of the chimera and the accumulation of free YFP in a less acidic environment. These results suggest that ABA-dependent induction of TSPO triggers the degradation of PIP2;7 through the autophagic pathway. To verify this interpretation, we incubated YFP-PIP2;7-expressing seedlings in ABA and monitored the levels of transgenic YFP-PIP2;7 and endogenous PIP2;7 by protein gel blotting at different time points. As shown in Figure 10, ABA-dependent induction of TSPO increased with time, while the levels of full-length transgenic YFP-PIP2;7 and that of endogenous PIP2;7 decreased steadily. We concluded that physiological levels of TSPO downregulate PIP2;7 through the autophagic pathway.

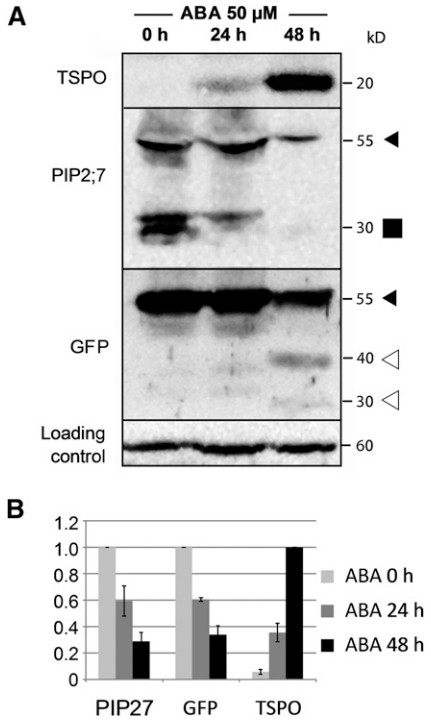

Figure 10. Physiological Levels of TSPO Induce the Degradation of Transgenic and Endogenous PIP2;7.

Transgenic *Arabidopsis* seedlings expressing YFP-PIP2;7 were incubated in 50 μM ABA and sampled at 0, 24, and 48 h time points. Total protein extractions were subjected to protein gel blotting and probed using anti-TSPO, anti-PIP2;7, and anti-GFP.

(A) The upper panel shows the time course induction of TSPO. The second panel shows the downregulation with time of transgenic YFP-PIP2;7 (filled arrowhead) and of the endogenous PIP2;7 (filled square). The third panel shows downregulation of the full-length YFP-PIP2;7 (filled arrowhead) and lower molecular size degradation products (open arrowheads) using anti-GFP.

(B) Relative quantification of the antigenic signals with the ratio at time 0 over the intensity of the corresponding loading control set as 1. TSPO increases with time and correlates with the decrease of the PIP2;7 signal. Bars represent the SE on the average of three measurements.

TSPO Abolishes the Cellular Water Transport Activity Induced by Overexpressed PIP2;7

The water transport activity of a given plant aquaporin can be assessed by overexpressing it in protoplasts and measuring the relative swelling of the transformed cells under hypotonic conditions (Besserer et al., 2012; Hachez et al., 2014). We prepared protoplasts from *Arabidopsis* seedlings overexpressing Venus-PIP2;7 in the wild type and in the TSPO-overexpressing backgrounds and compared their swelling (Figures 11A and 11B). After 45 s of incubation in the hypotonic solution, protoplasts expressing Venus-PIP2;7 alone were at least 10% larger in relative volume than those coexpressing Venus-PIP2;7 and TSPO (Figure 11A). We then compared the osmotic water permeability coefficient (P_f) of protoplasts prepared from wild-type seedlings (Columbia-0 [Col-0]), transgenic seedlings overexpressing TSPO (TSPO OE), and transgenic seedlings overexpressing Venus-PIP2;7 in the wild-type background (YFP-PIP2;7 Col0) or in the TSPO overexpression background (Venus-PIP2;7 TSPO OE). As shown in Figure 11B, protoplasts from seedlings expressing Venus-PIP2;7 in the wild-type background showed a 2-fold increase in their maximum P_f compared with control protoplasts from wild-type untransformed seedlings ($P < 0.0001$) or to those from TSPO-overexpressing seedlings ($P < 0.0001$). Interestingly, expression of Venus-PIP2;7 in the TSPO-overexpressing background had no effect on the maximum P_f of the resulting protoplasts, suggesting that the expression of TSPO abolishes the P_f increase generated by Venus-PIP2;7. In the presence of both Venus-PIP2;7 and TSPO, the mean maximum P_f of the protoplasts was not statistically different from the control (Col-0) protoplasts ($P = 0.38$) or the TSPO OE protoplasts ($P = 0.67$). Confocal imaging of Venus-PIP2;7 from the isolated protoplasts showed that although all of the cells from the wild-type

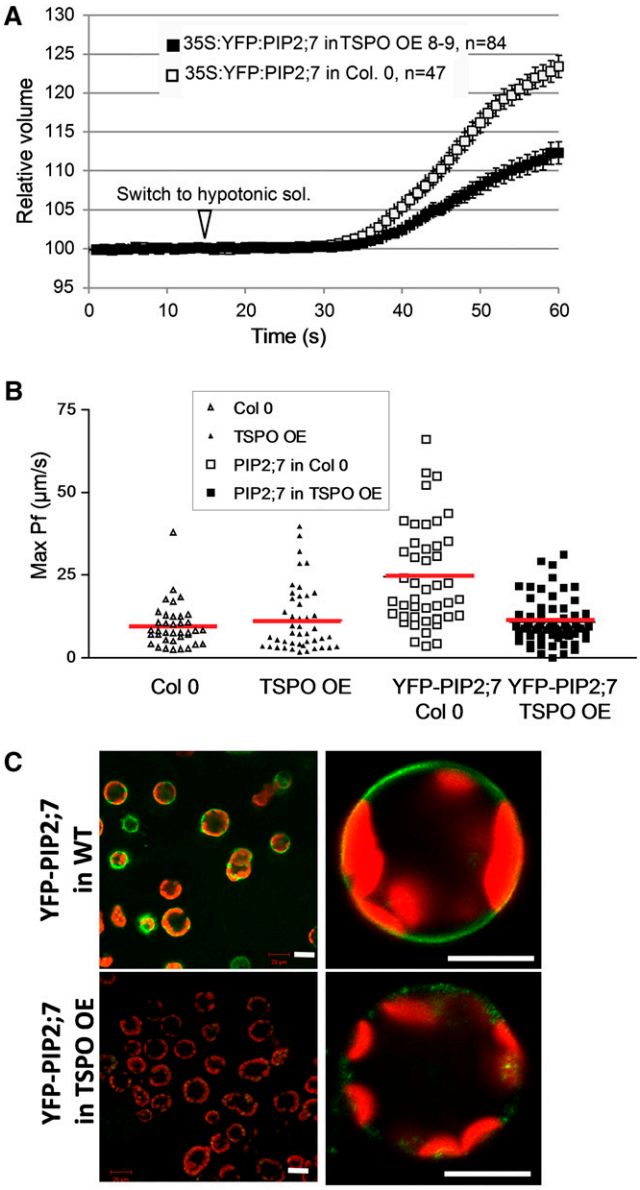

Figure 11. Overexpression of YFP-PIP2;7 Increases Leaf Protoplast Water Permeability, Which Is Annulled by Coexpressing TSPO.

(A) Time-lapse recording of the volume change of *Arabidopsis* mesophyll protoplasts overexpressing YFP-PIP2;7 in the wild-type *Arabidopsis* background (Col-0, white squares) or the TSPO background (mixture of protoplasts from two homozygous stable lines overexpressing TSPO OE8 and OE9, and TSPO OE 8-9; black squares). The cells were equilibrated for 15 s in an isotonic solution before switching (arrowhead) to a hypertonic solution for 45 s. The plotted values are the means from three independent experiments, and the error bars represent SE.

(B) Individual max P_f values of *Arabidopsis* mesophyll protoplasts from the wild type (Col-0), OE8 and OE9 transgenic lines overexpressing TSPO (TSPO OE), a transgenic line overexpressing YFP-PIP2;7 (YFP-PIP2;7 Col-0), and OE8 and OE9 expressing YFP-PIP2;7 (YFP-PIP2;7 TSPO OE). The red horizontal line defines the mean of the max P_f for each data set and was significantly ($P < 0.0001$) higher for YFP-PIP2;7 Col-0 compared with the other values.

(C) Confocal images of protoplasts as in **(A)** expressing YFP-PIP2;7 (green channel, chlorophylls red channel) in the wild-type background (upper panels) or in a background overexpressing TSPO (bottom panels). Coexpression of TSPO substantially reduces YFP-PIP2;7 fluorescence in the plasma membrane as exemplified by the magnified images of a single protoplast in the right hand panels. Bars = 10 μm in the left-hand panels and 20 μm in the right-hand panels.

background were fluorescent, <30% of the protoplasts from the TSPO overexpression background showed dimmed fluorescence (Figure 11C). In addition, while the fluorescence of Venus-PIP2;7 was mainly detected in the plasma membrane in the wild-type background (top right panel), in the TSPO background, very little fluorescence outlined the protoplast, but instead labeled the intracellular structures (bottom right panel). These results demonstrate that, when coexpressed, TSPO and PIP2;7 do interact and that this interaction partially prevents the targeting of PIP2;7 to the plasma membrane and consequently reduces the PIP2;7-dependent water transport of the cell.

In addition, a comparison of water loss suggests that detached leaves from transgenic OE8 plants lose less water than leaves from the wild-type or KO plants (Supplemental Figure 7A). Furthermore, seedlings of the overexpression H91A mutant seem to have even minimal further relative water loss compared with overexpression of the wild-type TSPO (on average <35% water loss for H91A-expressing seedlings compared with 54% for the OE8 line and >60% for wild-type seedlings after 2 h of incubation at room temperature; Supplemental Figure 7B). It is likely that the reduced water loss in the presence of TSPO is a consequence of TSPO-dependent downregulation of PIP2;7 and proceeds through a physical interaction between TSPO and PIP2;7, with the complex being targeted for degradation by the same selective autophagic pathway that downregulates TSPO. The H91A mutant form could still interact and retain intracellularly the PIP2;7 en route to the plasma membrane without significantly affecting the overall level of PIP2;7 in the cell.

DISCUSSION

In this work, we present evidence that the multi-stress-regulated membrane protein TSPO is involved in downregulation of a plasma membrane aquaporin, PIP2;7. We showed that TSPO interacts with PIP2;7 within membrane compartments of the early secretory pathway and that the heterocomplex is most likely targeted by the autophagic pathway for degradation in the vacuole, thus reducing the abundance of the PIP2;7 protein at the plasma membrane and protecting the cell from water deficit. Downregulation of PIP2;7 during water-related stress conditions may therefore be linked, at least in part, to the posttranslational regulation of induced TSPO by the plant cell.

Cell-Dependent Downregulation of Constitutively Expressed TSPO

We showed previously that overexpression of TSPO can be detrimental to the plant cell (Guillaumot et al., 2009). Cultured

cells constitutively expressing TSPO were more sensitive to salinity stress conditions, although they were more tolerant to osmotic stress conditions. More intriguing is the fact that it is impossible to maintain cell lines overexpressing TSPO for more than 6 months in the laboratory, suggesting that the continued presence of this protein in the cell is somehow toxic. It was shown that cultured cells overexpressing TSPO tend to accumulate relatively higher levels of reactive oxygen species, and this is likely due to the heme scavenging activity of this protein (Vanhee et al., 2011b). The data presented herein corroborate these earlier observations. We showed here that at the plant level, overexpressed TSPO failed to accumulate in most cells of various organs, possibly due to an intrinsic toxicity of the protein (Figure 4). Interestingly, TSPO from an *Arabidopsis* relative (*E. salsugineum*) showed the same behavior, suggesting that this regulatory mechanism is not a peculiarity of *Arabidopsis* TSPO. Downregulation of the expressed TSPO required heme binding, since the H91A mutant form seems to be relatively more stable than the wild-type form (Figure 6). Why the downregulation of overexpressed plant TSPOs appears to be less effective in some cells is not yet clear. A possible explanation is that it could be due to the differences in active ABA content and/or ABA-dependent signaling in different cell types. For instance, endogenous TSPO accumulates during seed maturation, a developmental stage coinciding with dehydration and ABA upregulation, but it disappears during imbibition of dry seeds, which triggers ABA degradation. We also consistently observed that in the leaf epidermis, YFP-TSPO was more commonly detected in the guard cells (although it was absent in the surrounding pavement cells) and along the veins, cell types known to be enriched in ABA biosynthetic genes and signaling components (Boursiac et al., 2013). ABA-dependent upregulation of the TSPO transcripts is at least 14-fold higher in the guard cells than in any other cell type of the leaf (26-fold increase in pavement cells compared with a 360-fold increase in guard cells) (Wang et al., 2011). It may be that the "dark" cells intrinsically possess an increased TSPO degradation rate (and codegradation of the complex containing PIP2;7). Alternatively, we speculate that the relative level or degradation kinetic of TSPO may explain that of PIP2;7. It may be that the expressed endogenous TSPO (because of differential ABA content and/or signaling) protein competes for degradation with the transgene product.

The Level and Activity of Aquaporins in the Plasma Membrane Are Regulated during Water-Related Stress

Plants have evolved complex physiological and biochemical mechanisms to adjust and adapt to environmental stresses. When subjected to abiotic stresses, such as salinity or drought stress, resulting in osmotic stress at the cellular level, plants actively reprogram their growth by modulating both cell division and cell expansion. One of the earliest metabolic responses to abiotic stresses and the inhibition of growth is the inhibition of protein synthesis and an increase in protein folding and processing. Growth is limited by the plant's ability to osmotically adjust or conduct water. Among the different families of aquaporins, the plasma membrane-localized PIPs appear to function in intercellular water transport. Continued cell-to-cell water transport during water-related stress can be detrimental to the plant. To date, the molecular identities of hyperosmotic sensors remain elusive in plants, but it is known that in general, the cell reacts to osmotic stress by reducing the number of water channels at the plasma membrane. PIP2;7 is one of the highly expressed plasma membrane aquaporins in the *Arabidopsis* rosette leaf (Prado et al., 2013). Aquaporin abundance and activity within the plasma membrane can be regulated by phosphorylation (Johansson et al., 1998; Prak et al., 2008; Van Wilder et al., 2008). Dephosphorylation of the loop B and/or C-terminal serine residues of PIP2s are predicted to stabilize the closed conformation of the water channels (Törnroth-Horsefield et al., 2006). In addition, the phosphorylation status

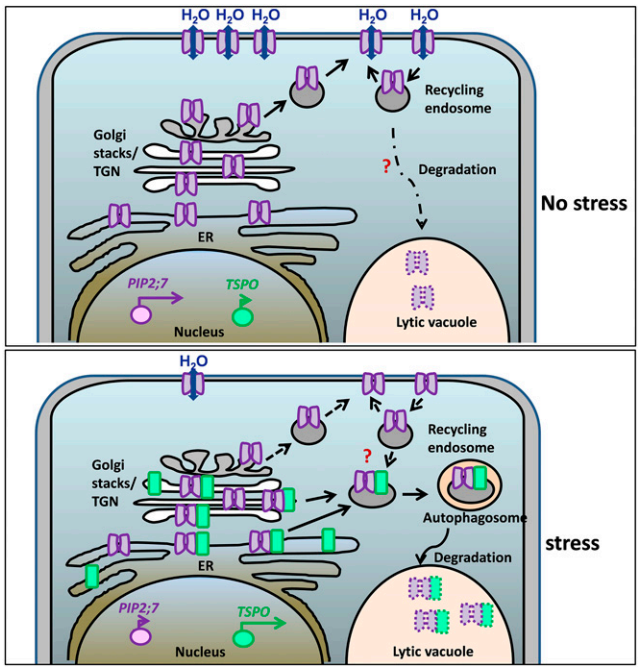

Figure 12. Hypothetical Model of PIP2;7 Downregulation by TSPO during Abiotic Stress.

In the absence of abiotic stress (upper panel), the level of TSPO is very low, as expressed TSPO is undetectable, while expressed PIP2;7 is targeted to the plasma membrane via the biosynthetic pathway and is involved in water transport activity. Under normal conditions, long-term PIP2;7 regulation could involve recycling via the endosome and vacuolar degradation. In the presence of abiotic stress conditions (bottom panel) involving increased ABA levels in the plant cell, TSPO is transcriptionally upregulated and the TSPO that is transiently synthesized is targeted to the Golgi via the ER, while downregulation of PIP2;7 is a means to limit intercellular water transport and prevent the dehydration of cells. To reduce the level of PIP2;7 in the plasma membrane, prevention of already translated PIP2;7 from reaching the plasma membrane (interrupted arrows) could involve titration of the water channel molecules present in the ER and/or the Golgi by TSPO through protein-protein interaction and vacuolar degradation of the complex via the autophagic pathway. The autophagic degradation of PIP2;7 and the endosomal pathway could come together (question mark), allowing the simultaneous cleansing of excess PIP2;7 from the plasma membrane and internal membranes.

of the C-terminal serine residues also regulates the abundance of PIPs in the plasma membrane in response to salt stress conditions (Prak et al., 2008). Internalization of *Arabidopsis* PIP2;1 involves two pathways: a tyrphostin A23-sensitive clathrin-dependent pathway and a methyl-β-cyclodextrin-sensitive, membrane raft-associated pathway (Li et al., 2011). Recently, it was shown that ABA can decrease the phosphorylation of PIP2;7 by up to 26% within 5 min of incubation of plant tissues in 50 μM ABA and can result in a 60% decrease after 30 min of incubation (Kline et al., 2010). Only four of the *Arabidopsis* plasma membrane aquaporins seem to be affected by these changes, and with different kinetics, suggesting that the ABA-dependent regulation is isoform dependent. ABA-dependent PIP2;7 dephosphorylation at a defined C-terminal site might inactivate the channel and trigger its internalization either for recycling or degradation through the vacuolar pathway. To be physiologically efficient, this process should be coupled to a mechanism preventing new PIP2;7 channel molecules from reaching the plasma membrane.

TSPO Interacts with and Acts as a Transient Regulator of PIP2;7

Transcriptional regulation suggests that TSPO and PIP2;7 are mutually exclusive throughout plant development. We found that when coexpressed, TSPO and PIP2;7 do interact, most likely in the ER and Golgi membrane. This interaction is physiologically relevant as it triggers the reduction of PIP2;7 channels present in the plasma membrane, as well as reduced water transport activity (Figure 11). Reduction of the abundance of aquaporins in the plasma membrane through protein-protein interaction within the cell has already been described in plants and in other cell types. The ER-localized E3 ubiquitin ligase Rma1H1 is induced by various abiotic stresses, and it inhibits the trafficking of PIP2;1 to the plasma membrane and targets the aquaporin for proteasomal degradation as a response to dehydration (Lee et al., 2009). AQPΔ4 is an alternative spliced variant of the human aquaporin AQP4 lacking exon 4 that exhibits no water activity and is retained in the ER (De Bellis et al., 2014). When AQPΔ4 is expressed in the presence of functional AQP4, the surface expression of the full-length protein is reduced, and water activity at the plasma membrane is diminished in comparison to cells expressing AQP4 alone. AQPΔ4 forms dimers with AQP4 in the ER and targets the complex for proteasomal degradation, therefore acting as a dominant-negative regulator (De Bellis et al., 2014). It seems that, at least for some plasma membrane aquaporins, protein-protein interaction and downregulation of the complex is a common regulatory mechanism although the regulator and pathway may vary.

Abiotic stress conditions enhance, at least temporally, autophagy in the plant cell (Bassham et al., 2006; Bassham, 2007; Liu and Bassham, 2012), probably through ABA-dependent inhibition of the target of rapamycin (TOR) kinase (Deprost et al., 2007; Liu and Bassham, 2010), a key macroautophagy regulator in eukaryotic cells. We found that pharmacological inhibition of the autophagic pathway stabilizes TSPO and concomitantly stabilizes PIP2;7, suggesting that both proteins not only interact but are also likely degraded through the same pathway. Consistent with this interpretation, the genetically stabilized form of TSPO harboring the H91A point mutation seems to have little or no effect on the level of endogenous PIP2;7, indicating that if the mutant form of TSPO is still able to interact with PIP2;7, the interaction is not conducive to degradation of the aquaporin. It would be interesting to investigate whether the TSPO/PIP2;7 interaction is affected by heme binding to TSPO. TSPO is actively degraded in the plant cell by a selective autophagic pathway (Vanhee et al., 2011b; Veljanovski and Batoko, 2014). We confirm here that TSPO physically interacts with ATG8, but it is not yet clear whether the interacting ATG8 molecules are membrane-bound or soluble. It is possible that TSPO acts as a selective autophagy receptor (Veljanovski and Batoko, 2014) and could initiate the recruitment of the autophagosome formation machinery through ATG8 binding or by interacting with phagophore-bound ATG8. Where and how the TSPO/PIP2;7 complex is selectively engulfed in autophagosomes remains to be determined.

TSPO, when expressed, could act as a negative regulator of PIP2;7 (Figure 12). The regulation of water transport by aquaporins may occur through modulating the gating (Törnroth-Horsefield et al., 2006) or alternatively by influencing the number of active channel molecules in the plasma membrane. The latter can be achieved by direct regulation of the expression of a given aquaporin gene and/or aquaporin trafficking and degradation (Boursiac et al., 2005, 2008; Lee et al., 2009; Besserer et al., 2012). Shutting down the transcription of the gene may not be enough, since the cell has to deal with translated molecules en route to the plasma membrane and what is already active in the plasma membrane (Figure 12). Transient titration of PIP2;7 by TSPO and subsequent degradation through the autophagic pathway could efficiently contribute to limiting tissue dehydration during exposure to stress conditions.

METHODS

Genetic Constructs and Transformations

Standard molecular biology protocols were followed, the plasmids generated were amplified in *Escherichia coli* strain DH5α, and all coding sequences were validated by sequencing.

The cDNAs of PIP2;7 and TSPO were amplified by PCR from a cDNA pool obtained by reverse transcription of mRNA from *Arabidopsis thaliana* Col-0 plants (for PIP2;7) or from the RIKEN clones RAFL09-68-G14 and RAFL05-18-I12 (Guillaumot et al., 2009) using the primer pairs U-PIP2;7 (5′-GGCTTAAUATGTCGAAAGAAGTGAGC-3′) and PIP2;7U (5′-GGTTTAA-UTTAATTGGTTGCGTTGCT-3′) or U-TSPO (5′-GGCTTAAUATGGATTCT-CAGGACATC-3′) and TSPO-U (5′-GGTTTAAUTCACGCGACTGCAAGCTT-3′), respectively. The PCR products were directionally cloned using a uracil excision-based improved high-throughput USER cloning technique (Nour-Eldin et al., 2006) into the USER-compatible vectors pCambia 3300-35S-Nterm-Y155N-u (Nour-Eldin et al., 2006) and pCambia-3300-35S-Nterm-Y155C-u (Nour-Eldin et al., 2006). The pCambia-3300-35S-Nterm-Y155N-u vector contains the cDNA encoding the first 155 amino acid residues of the YFP-derivative Venus (Nagai et al., 2002), followed by a sequence encoding a linker consisting of Gly-Ser-Gly-Gly-Leu-Arg-Leu-Asn. The pCambia-3300-35S-Nterm-Y155C-u vector contains the cDNA encoding the last 91 amino acid residues of the YFP-derivative Venus followed by the same sequence encoding the linker described above. The cDNAs encoding PIP2;7 and TSPO were inserted into these vectors to express them fused to the split Venus ($Venus^N$-PIP2:7, $Venus^C$-PIP2;7, $Venus^N$-TSPO, and

Venus^{C}-PIP2;7). The USER-cloning compatible PCR fragment encoding either PIP2;7 or TSPO was also cloned into the binary vector pCambia-2300-35S-N-term-CFP-u or pCambia-3300-35S-N-term-YFP-u, allowing the expression of PIP2;7 or TSPO N-terminally fused to monomeric CFP or YFP/Venus. The *Thellungiella salsuginea* (*Eutrema salsugineum*) TSPO (Ts-TSPO) cDNA was obtained from RIKEN (clones pdh08542 and pdh04089). The binary vector pCambia-YFP-TsTSPO was obtained using the same cloning strategy as described for generating pCambia-YFP-AtTSPO (Guillaumot et al., 2009), except that the primer BamHIThTSPO 5′-TTTTGGATCCTCACGCGATTG-CAAGC-3′ was used as a 3′ primer for PCR amplification of the Ts-TSPO coding sequence. Although the pdh04089 clone contains a single nucleotide polymorphic mutation, compared with the construct containing the pdh08542 clone, this did not affect the expression and subcellular localization of the fusion protein. For the generation of mCherry-GFP coupled to the At-TSPO variants, the following primers were used in overlapping PCRs: CGF1 (5′-AAAAAGCTTATGGTGAGCAAGGGCAGGAG-3′) and CGR1 (5′-CTTTACTCATTCCCGCTCCCGCTCCCGCCTTGTACAGCTCGTC-CATG-3′) to amplify mCherry, CGF2 (5′-GCTGTACAAGGCGG-GAGCGGGAGCGGGAATGAGTAAAGGAGAAGAAC-3′) and CGR2 (5′-TTTCTAGATTTGTATAGTTCATCCATGCCA-3′) to amplify GFP from pVKH18-En6-ST-GFP (Batoko et al., 2000; Saint-Jore et al., 2002), FTSPO (5′-GGGGTCTAGAGGAGCTGGTGGAGCTGGTGGAGCTGTAT-GGACTCTCAG-3′) and RTSPO (5′-GGGGAGATCTGTCGACTCACG-CACTGCAAG-3′) to amplify At-TSPO variants from p426GAL1-AtTSPO and p426GAL1-AtTSPO^{H91A} (Vanhee et al., 2011b). The final PCR product encoding mCherry-GFP was digested with *Hin*dIII and *Xba*I and cloned into pPILY, which was digested with the same restriction enzymes. The At-TSPO variants were cloned downstream of the mCherry-GFP using *Xba*I and *Bgl*II. The expression cassette containing a double p35S promoter was retrieved from pPILY using *Not*I and subcloned into pAUX-3131 opened with *Not*I, then into the binary vector pMODUL using I-SCEI (Goderis et al., 2002). To generate RFP-TSPO, the coding sequence of TSPO was PCR amplified using the primers TSPO_D-topoF, 5′-CACCATGGATTCTCAG-GACATCAGATAC-3′, and TSPO_D-topoR, 5′-TCACGCGACTGCAAGCTT-TACATTAA-3′, and the PCR product was inserted into pUBN-RFP-DEST (Grefen et al., 2010) following the Gateway cloning procedure as described by the supplier. The generation of stable transgenic *Arabidopsis* plant lines expressing At-TSPO (OE8 and OE9) or YFP-At-TSPO, YFP-PIP2;7, and CFP-PIP2;7 has been described (Guillaumot et al., 2009; Vanhee et al., 2011b; Hachez et al., 2014), and the same procedure was followed to obtain transgenic lines expressing YFP-Ts-TSPO, mCherry-GFP-At-TSPO, and mCherry-GFP-At-TSPO^{H91A}. Transient expression in *Nicotiana tabacum* was performed essentially as described (Batoko et al., 2000).

Split-Ubiquitin Screen

The split-ubiquitin screen was conducted using the full-length At-TSPO as bait and performed by the commercial firm Dualsystems Biotech. The bait construct for screening was made by PCR amplification of the cDNA encoding TSPO from the RIKEN clones RAFL09-68-G14 and RAFL05-18-I12 and cloned using the *Sfi*I sites in the pBT3-N and pBT3-SUC vectors (Dualsystems Biotech) to generate pBT3-N-AtTSPO and pBT3-SUC-AtTSPO encoding a fusion protein with VP16-LexA-Cub fused to the N terminus or the C terminus of TSPO, respectively. In addition to the TSPO coding region, the 5′ and 3′ junctions were further examined by sequencing. The bait constructs were transformed into the NMY32 strain [MATa his3delta200 trp1-901 leu2-3 112 ADE2:(lexAop)$_8$-ADE2 LYS2:(lexAop)$_4$-HIS3 URA3:(lexAop)$_8$-lacZ GAL4] using standard procedures (Gietz and Woods, 2001). Correct expression of the bait was verified by protein gel blotting of cell extracts using mouse monoclonal antibodies directed against the LexA domain (Santa Cruz Biotechnology). The absence of self-activation was verified by cotransformation of the bait together with several control preys (from different subcellular compartments) and selection on minimal medium lacking tryptophan, leucine, histidine, and adenine (selective medium). The bait was cotransformed sequentially together with an *Arabidopsis* cDNA library in the pDSL-Nx vector (complexity of the library 1.7×10^7, average insert size 1.7 kb). Positive transformants were tested for β-galactosidase activity using a high-throughput plate-based assay (Möckli and Auerbach, 2004). All of the initial positive transformants showed β-galactosidase activity and were considered true positives.

Plant Material and Treatments

Disinfection of *Arabidopsis* seeds, plant growth conditions, and ABA treatment were performed as described by Guillaumot et al. (2009). The isolation and analysis of mesophyll protoplasts were as described by Hachez et al. (2014). ConcA treatment were conducted as described (Vanhee et al., 2011b) and roots imaged after 24 h. Plant tissue dehydration assays were conducted as described (Cao et al., 2013).

Protein Extraction and Analyses

Plant protein extraction and preparation and solubilization of microsomes were conducted as previously described (Vanhee et al., 2011a, 2011b). GFP-Trap and RFP-trap (Chromotek) pull-down assays were conducted according to the manufacturer's instructions and adapted to our materials as previously described (Hachez et al., 2014). Protein electrophoresis, protein gel blotting, and signal quantifications were performed as described by Guillaumot et al. (2009). For ATG8 detection, electrophoresis and protein gel blotting were as described by Kwon et al. (2010). Antibody against actin was purchased from Santa Cruz Biotechnology, anti-PIP2;7, anti-*Arabidopsis* RbcL, and Lhcb1 were purchased from AgriSera, and anti-*Arabidopsis* ATG8 was a generous gift of K.P. Okhmae (School of Life Sciences and Biotechnology, Korea University, Seoul). Anti-TSPO and anti-GFP/YFP have been described previously and were used accordingly (Guillaumot et al., 2009). Horseradish peroxidase-coupled anti-rabbit and anti-mouse secondary antibody were from Sigma-Aldrich and were used at 1:10,000.

Cell Imaging

Confocal imaging using a Zeiss LSM710 confocal microscope equipped with a spectral detector was performed as described (Guillaumot et al., 2009; Vanhee et al., 2011a, 2011b; Hachez et al., 2014). Identical settings, including optical section thickness, were thoroughly used during the acquisition for sample comparison, and the images processed using identical parameters. When YFP and GFP fusion proteins were imaged simultaneously, the 458-nm laser was used to excite GFP and the amplified emitted light was recorded between 463 and 510 nm. YFP fluorophores were simultaneously excited with a 514-nm argon multiline laser and the amplified emitted light was recorded between 520 and 610 nm. RFP fluorophores were excited with a 561-nm laser and the amplified emitted light was recorded between 570 and 635 nm. The confocal images were processed using Imaris software (Bitplane). Cells were manually scored for the presence or absence of fluorescence from randomly imaged sections.

Statistical Analysis of the Data

Statistical analysis was conducted using GraphPad Prism software, version 3.00, to determine the significance of the presented data.

Accession Numbers

Sequence data from this article can be found in the GenBank/EMBL data libraries and in the Arabidopsis Genome Initiative genome databases under the following accession numbers: At2g47770 (At-TSPO), At4g35100 (PIP2;7), and AK352924.1 (Ts-TSPO).

Supplemental Data

The following materials are available in the online version of this article.

Supplemental Figure 1. Results of the Commercial Screening of the At-TSPO Interactants Using the Split Ubiquitin Technique.

Supplemental Figure 2. Comparative Transcriptional Regulation of *Arabidopsis* TSPO and PIP2;7.

Supplemental Figure 3. Time-Course Expression of PIP2;7 and TSPO during Seed Imbibition and Germination.

Supplemental Figure 4. Technical Controls for Figure 2.

Supplemental Figure 5. Expression Pattern of YFP-PIP2;7 in the Segregating Population Coexpressing TSPO.

Supplemental Figure 6. UBI10-Driven Expression of RFP-TSPO Shows a Patchy Distribution of RFP Fluorescence.

Supplemental Figure 7. Relative Water Loss from Various At-TSPO Mutants.

ACKNOWLEDGMENTS

We thank K.P. Okhmae (School of Life Sciences and Biotechnology, Korea University, Seoul), C. Grefen (ZMBP Developmental Genetics, University of Tuebingen, Germany), M.R. Blatt (Laboratory of Plant Physiology and Biophysics, University of Glasgow, UK), RIKEN, ABRC, and the Nottingham Arabidopsis Stock Centre for providing reagents or plant materials. We also thank N. Nigam for generating mCherry-GFP-TSPO transgenic lines and the data presented in Supplemental Figure 3 and D. Masquelier for technical assistance. Confocal microscopy was carried out at the UCL imaging platform IMABIOL. This work was partly funded by the Interuniversity Attraction Poles Programme–Belgian Science Policy, the Fédération Wallonie-Bruxelles-Actions de Recherches Concertées, and the Belgian Funds for Scientific Research (FNRS). C.H. was a FNRS postdoctoral researcher, and H.B. is a Research Associate of the FRS-FNRS.

AUTHOR CONTRIBUTIONS

C.H., C.V., F.C., and H.B. conceived and designed the experiments. C.H., V.V., C.V., H.R., D.G., and H.B. performed the experiments. C.H., V.V., F.C., and H.B. analyzed the data. H.B. supervised the research and wrote the article with input from all the coauthors.

Received November 6, 2014; revised November 27, 2014; accepted December 3, 2014; published December 23, 2014.

REFERENCES

Alexandersson, E., Danielson, J.A., Råde, J., Moparthi, V.K., Fontes, M., Kjellbom, P., and Johanson, U. (2010). Transcriptional regulation of aquaporins in accessions of Arabidopsis in response to drought stress. Plant J. **61:** 650–660.

Bassham, D.C. (2007). Plant autophagy—more than a starvation response. Curr. Opin. Plant Biol. **10:** 587–593.

Bassham, D.C., Laporte, M., Marty, F., Moriyasu, Y., Ohsumi, Y., Olsen, L.J., and Yoshimoto, K. (2006). Autophagy in development and stress responses of plants. Autophagy **2:** 2–11.

Batoko, H., Zheng, H.Q., Hawes, C., and Moore, I. (2000). A rab1 GTPase is required for transport between the endoplasmic reticulum and Golgi apparatus and for normal Golgi movement in plants. Plant Cell **12:** 2201–2218.

Besserer, A., Burnotte, E., Bienert, G.P., Chevalier, A.S., Errachid, A., Grefen, C., Blatt, M.R., and Chaumont, F. (2012). Selective regulation of maize plasma membrane aquaporin trafficking and activity by the SNARE SYP121. Plant Cell **24:** 3463–3481.

Boursiac, Y., Boudet, J., Postaire, O., Luu, D.T., Tournaire-Roux, C., and Maurel, C. (2008). Stimulus-induced downregulation of root water transport involves reactive oxygen species-activated cell signalling and plasma membrane intrinsic protein internalization. Plant J. **56:** 207–218.

Boursiac, Y., Chen, S., Luu, D.T., Sorieul, M., van den Dries, N., and Maurel, C. (2005). Early effects of salinity on water transport in Arabidopsis roots. Molecular and cellular features of aquaporin expression. Plant Physiol. **139:** 790–805.

Boursiac, Y., Léran, S., Corratgé-Faillie, C., Gojon, A., Krouk, G., and Lacombe, B. (2013). ABA transport and transporters. Trends Plant Sci. **18:** 325–333.

Bracha-Drori, K., Shichrur, K., Katz, A., Oliva, M., Angelovici, R., Yalovsky, S., and Ohad, N. (2004). Detection of protein-protein interactions in plants using bimolecular fluorescence complementation. Plant J. **40:** 419–427.

Braestrup, C., Albrechtsen, R., and Squires, R.F. (1977). High densities of benzodiazepine receptors in human cortical areas. Nature **269:** 702–704.

Cao, M., et al. (2013). An ABA-mimicking ligand that reduces water loss and promotes drought resistance in plants. Cell Res. **23:** 1043–1054.

Chaumont, F., and Tyerman, S.D. (2014). Aquaporins: highly regulated channels controlling plant water relations. Plant Physiol. **164:** 1600–1618.

Corsi, L., Avallone, R., Geminiani, E., Cosenza, F., Venturini, I., and Baraldi, M. (2004). Peripheral benzodiazepine receptors in potatoes (*Solanum tuberosum*). Biochem. Biophys. Res. Commun. **313:** 62–66.

De Bellis, M., Pisani, F., Mola, M.G., Basco, D., Catalano, F., Nicchia, G.P., Svelto, M., and Frigeri, A. (2014). A novel human aquaporin-4 splice variant exhibits a dominant-negative activity: a new mechanism to regulate water permeability. Mol. Biol. Cell **25:** 470–480.

Deprost, D., Yao, L., Sormani, R., Moreau, M., Leterreux, G., Nicolaï, M., Bedu, M., Robaglia, C., and Meyer, C. (2007). The Arabidopsis TOR kinase links plant growth, yield, stress resistance and mRNA translation. EMBO Rep. **8:** 864–870.

Fan, J., Rone, M.B., and Papadopoulos, V. (2009). Translocator protein 2 is involved in cholesterol redistribution during erythropoiesis. J. Biol. Chem. **284:** 30484–30497.

Fetter, K., Van Wilder, V., Moshelion, M., and Chaumont, F. (2004). Interactions between plasma membrane aquaporins modulate their water channel activity. Plant Cell **16:** 215–228.

Finkelstein, R. (2013). Abscisic acid synthesis and response. The Arabidopsis Book **11:** e0166, doi/10.1199/tab.0166.

Finkelstein, R.R., Gampala, S.S.L., and Rock, C.D. (2002). Abscisic acid signaling in seeds and seedlings. Plant Cell **14** (Suppl): S15–S45.

Frank, W., Baar, K.M., Qudeimat, E., Woriedh, M., Alawady, A., Ratnadewi, D., Gremillon, L., Grimm, B., and Reski, R. (2007). A mitochondrial protein homologous to the mammalian peripheral-type benzodiazepine receptor is essential for stress adaptation in plants. Plant J. **51:** 1004–1018.

Fujii, H., and Zhu, J.K. (2009). Arabidopsis mutant deficient in 3 abscisic acid-activated protein kinases reveals critical roles in growth, reproduction, and stress. Proc. Natl. Acad. Sci. USA **106:** 8380–8385.

Fujita, M., Fujita, Y., Noutoshi, Y., Takahashi, F., Narusaka, Y., Yamaguchi-Shinozaki, K., and Shinozaki, K. (2006). Crosstalk between abiotic and biotic stress responses: a current view from

the points of convergence in the stress signaling networks. Curr. Opin. Plant Biol. **9:** 436–442.

Gavish, M., Bachman, I., Shoukrun, R., Katz, Y., Veenman, L., Weisinger, G., and Weizman, A. (1999). Enigma of the peripheral benzodiazepine receptor. Pharmacol. Rev. **51:** 629–650.

Gietz, R.D., and Woods, R.A. (2002). Transformation of yeast by lithium acetate/single-stranded carrier DNA/polyethylene glycol method. Methods Enzymol. **350:** 87–96.

Goderis, I.J., De Bolle, M.F., François, I.E., Wouters, P.F., Broekaert, W.F., and Cammue, B.P. (2002). A set of modular plant transformation vectors allowing flexible insertion of up to six expression units. Plant Mol. Biol. **50:** 17–27.

Grefen, C., Donald, N., Hashimoto, K., Kudla, J., Schumacher, K., and Blatt, M.R. (2010). A ubiquitin-10 promoter-based vector set for fluorescent protein tagging facilitates temporal stability and native protein distribution in transient and stable expression studies. Plant J. **64:** 355–365.

Guillaumot, D., Guillon, S., Déplanque, T., Vanhee, C., Gumy, C., Masquelier, D., Morsomme, P., and Batoko, H. (2009). The Arabidopsis TSPO-related protein is a stress and abscisic acid-regulated, endoplasmic reticulum-Golgi-localized membrane protein. Plant J. **60:** 242–256.

Hachez, C., Laloux, T., Reinhardt, H., Cavez, D., Degand, H., Grefen, C., De Rycke, R., Inzé, D., Blatt, M.R., Russinova, E., and Chaumont, F. (2014). Arabidopsis SNAREs SYP61 and SYP121 coordinate the trafficking of plasma membrane aquaporin PIP2;7 to modulate the cell membrane water permeability. Plant Cell **26:** 3132–3147.

Hermans, C., Vuylsteke, M., Coppens, F., Craciun, A., Inzé, D., and Verbruggen, N. (2010). Early transcriptomic changes induced by magnesium deficiency in *Arabidopsis thaliana* reveal the alteration of circadian clock gene expression in roots and the triggering of abscisic acid-responsive genes. New Phytol. **187:** 119–131.

Jang, J.Y., Kim, D.G., Kim, Y.O., Kim, J.S., and Kang, H. (2004). An expression analysis of a gene family encoding plasma membrane aquaporins in response to abiotic stresses in *Arabidopsis thaliana.* Plant Mol. Biol. **54:** 713–725.

Javot, H., Lauvergeat, V., Santoni, V., Martin-Laurent, F., Güçlü, J., Vinh, J., Heyes, J., Franck, K.I., Schäffner, A.R., Bouchez, D., and Maurel, C. (2003). Role of a single aquaporin isoform in root water uptake. Plant Cell **15:** 509–522.

Johansson, I., Karlsson, M., Shukla, V.K., Chrispeels, M.J., Larsson, C., and Kjellbom, P. (1998). Water transport activity of the plasma membrane aquaporin PM28A is regulated by phosphorylation. Plant Cell **10:** 451–459.

Joo, H.K., Lee, Y.R., Lim, S.Y., Lee, E.J., Choi, S., Cho, E.J., Park, M.S., Ryoo, S., Park, J.B., and Jeon, B.H. (2012). Peripheral benzodiazepine receptor regulates vascular endothelial activations via suppression of the voltage-dependent anion channel-1. FEBS Lett. **586:** 1349–1355.

Kline, K.G., Barrett-Wilt, G.A., and Sussman, M.R. (2010). *In planta* changes in protein phosphorylation induced by the plant hormone abscisic acid. Proc. Natl. Acad. Sci. USA **107:** 15986–15991.

Kreps, J.A., Wu, Y., Chang, H.S., Zhu, T., Wang, X., and Harper, J.F. (2002). Transcriptome changes for Arabidopsis in response to salt, osmotic, and cold stress. Plant Physiol. **130:** 2129–2141.

Kwon, S.I., Cho, H.J., Jung, J.H., Yoshimoto, K., Shirasu, K., and Park, O.K. (2010). The Rab GTPase RabG3b functions in autophagy and contributes to tracheary element differentiation in Arabidopsis. Plant J. **64:** 151–164.

Lacapère, J.J., and Papadopoulos, V. (2003). Peripheral-type benzodiazepine receptor: structure and function of a cholesterol-binding protein in steroid and bile acid biosynthesis. Steroids **68:** 569–585.

Lee, H.K., Cho, S.K., Son, O., Xu, Z., Hwang, I., and Kim, W.T. (2009). Drought stress-induced Rma1H1, a RING membrane-anchor E3 ubiquitin ligase homolog, regulates aquaporin levels via ubiquitination in transgenic Arabidopsis plants. Plant Cell **21:** 622–641.

Li, X., Wang, X., Yang, Y., Li, R., He, Q., Fang, X., Luu, D.T., Maurel, C., and Lin, J. (2011). Single-molecule analysis of PIP2;1 dynamics and partitioning reveals multiple modes of Arabidopsis plasma membrane aquaporin regulation. Plant Cell **23:** 3780–3797.

Lindemann, P., Koch, A., Degenhardt, B., Hause, G., Grimm, B., and Papadopoulos, V. (2004). A novel *Arabidopsis thaliana* protein is a functional peripheral-type benzodiazepine receptor. Plant Cell Physiol. **45:** 723–733.

Liu, J., et al. (2011). Beclin1 controls the levels of p53 by regulating the deubiquitination activity of USP10 and USP13. Cell **147:** 223–234.

Liu, Y., and Bassham, D.C. (2010). TOR is a negative regulator of autophagy in *Arabidopsis thaliana.* PLoS ONE **5:** e11883.

Liu, Y., and Bassham, D.C. (2012). Autophagy: pathways for self-eating in plant cells. Annu. Rev. Plant Biol. **63:** 215–237.

Ma, Y., Szostkiewicz, I., Korte, A., Moes, D., Yang, Y., Christmann, A., and Grill, E. (2009). Regulators of PP2C phosphatase activity function as abscisic acid sensors. Science **324:** 1064–1068.

Maurel, C., Verdoucq, L., Luu, D.T., and Santoni, V. (2008). Plant aquaporins: membrane channels with multiple integrated functions. Annu. Rev. Plant Biol. **59:** 595–624.

Mlotshwa, S., Pruss, G.J., Gao, Z., Mgutshini, N.L., Li, J., Chen, X., Bowman, L.H., and Vance, V. (2010). Transcriptional silencing induced by Arabidopsis T-DNA mutants is associated with 35S promoter siRNAs and requires genes involved in siRNA-mediated chromatin silencing. Plant J. **64:** 699–704.

Möckli, N., and Auerbach, D. (2004). Quantitative beta-galactosidase assay suitable for high-throughput applications in the yeast two-hybrid system. Biotechniques **36:** 872–876.

Morohaku, K., Pelton, S.H., Daugherty, D.J., Butler, W.R., Deng, W., and Selvaraj, V. (2014). Translocator protein/peripheral benzodiazepine receptor is not required for steroid hormone biosynthesis. Endocrinology **155:** 89–97.

Nagai, T., Ibata, K., Park, E.S., Kubota, M., Mikoshiba, K., and Miyawaki, A. (2002). A variant of yellow fluorescent protein with fast and efficient maturation for cell-biological applications. Nat. Biotechnol. **20:** 87–90.

Nambara, E., and Marion-Poll, A. (2005). Abscisic acid biosynthesis and catabolism. Annu. Rev. Plant Biol. **56:** 165–185.

Nour-Eldin, H.H., Hansen, B.G., Nørholm, M.H., Jensen, J.K., and Halkier, B.A. (2006). Advancing uracil-excision based cloning towards an ideal technique for cloning PCR fragments. Nucleic Acids Res. **34:** e122.

Papadopoulos, V., Baraldi, M., Guilarte, T.R., Knudsen, T.B., Lacapère, J.J., Lindemann, P., Norenberg, M.D., Nutt, D., Weizman, A., Zhang, M.R., and Gavish, M. (2006). Translocator protein (18kDa): new nomenclature for the peripheral-type benzodiazepine receptor based on its structure and molecular function. Trends Pharmacol. Sci. **27:** 402–409.

Park, S.Y., et al. (2009). Abscisic acid inhibits type 2C protein phosphatases via the PYR/PYL family of START proteins. Science **324:** 1068–1071.

Postaire, O., Tournaire-Roux, C., Grondin, A., Boursiac, Y., Morillon, R., Schäffner, A.R., and Maurel, C. (2010). A PIP1 aquaporin contributes to hydrostatic pressure-induced water transport in both the root and rosette of Arabidopsis. Plant Physiol. **152:** 1418–1430.

Prado, K., Boursiac, Y., Tournaire-Roux, C., Monneuse, J.M., Postaire, O., Da Ines, O., Schäffner, A.R., Hem, S., Santoni, V., and Maurel, C. (2013). Regulation of Arabidopsis leaf hydraulics involves light-dependent phosphorylation of aquaporins in veins. Plant Cell **25:** 1029–1039.

Prak, S., Hem, S., Boudet, J., Viennois, G., Sommerer, N., Rossignol, M., Maurel, C., and Santoni, V. (2008). Multiple

phosphorylations in the C-terminal tail of plant plasma membrane aquaporins: role in subcellular trafficking of AtPIP2;1 in response to salt stress. Mol. Cell. Proteomics **7:** 1019–1030.

Rupprecht, R., Papadopoulos, V., Rammes, G., Baghai, T.C., Fan, J., Akula, N., Groyer, G., Adams, D., and Schumacher, M. (2010). Translocator protein (18 kDa) (TSPO) as a therapeutic target for neurological and psychiatric disorders. Nat. Rev. Drug Discov. **9:** 971–988.

Rupprecht, R., et al. (2009). Translocator protein (18 kD) as target for anxiolytics without benzodiazepine-like side effects. Science **325:** 490–493.

Saint-Jore, C.M., Evins, J., Batoko, H., Brandizzi, F., Moore, I., and Hawes, C. (2002). Redistribution of membrane proteins between the Golgi apparatus and endoplasmic reticulum in plants is reversible and not dependent on cytoskeletal networks. Plant J. **29:** 661–678.

Seglen, P.O., and Gordon, P.B. (1982). 3-Methyladenine: specific inhibitor of autophagic/lysosomal protein degradation in isolated rat hepatocytes. Proc. Natl. Acad. Sci. USA **79:** 1889–1892.

Seki, M., et al. (2002). Monitoring the expression profiles of 7000 Arabidopsis genes under drought, cold and high-salinity stresses using a full-length cDNA microarray. Plant J. **31:** 279–292.

Shang, Y., et al. (2010). The Mg-chelatase H subunit of Arabidopsis antagonizes a group of WRKY transcription repressors to relieve ABA-responsive genes of inhibition. Plant Cell **22:** 1909–1935.

Sileikyte, J., Blachly-Dyson, E., Sewell, R., Carpi, A., Menabo, R., Di Lisa, F., Ricchelli, F., Bernardi, P., and Forte, M. (2014). Regulation of the mitochondrial permeability transition pore by the outer membrane does not involve the peripheral benzodiazepine receptor (TSPO). J. Biol. Chem. **289:** 13769–13781.

Stocco, D.M. (2014). The role of PBR/TSPO in steroid biosynthesis challenged. Endocrinology **155:** 6–9.

Törnroth-Horsefield, S., Wang, Y., Hedfalk, K., Johanson, U., Karlsson, M., Tajkhorshid, E., Neutze, R., and Kjellbom, P. (2006). Structural mechanism of plant aquaporin gating. Nature **439:** 688–694.

Van Wilder, V., Miecielica, U., Degand, H., Derua, R., Waelkens, E., and Chaumont, F. (2008). Maize plasma membrane aquaporins belonging to the PIP1 and PIP2 subgroups are *in vivo* phosphorylated. Plant Cell Physiol. **49:** 1364–1377.

Vanhee, C., Guillon, S., Masquelier, D., Degand, H., Deleu, M., Morsomme, P., and Batoko, H. (2011a). A TSPO-related protein localizes to the early secretory pathway in Arabidopsis, but is targeted to mitochondria when expressed in yeast. J. Exp. Bot. **62:** 497–508.

Vanhee, C., Zapotoczny, G., Masquelier, D., Ghislain, M., and Batoko, H. (2011b). The Arabidopsis multistress regulator TSPO is a heme binding membrane protein and a potential scavenger of porphyrins via an autophagy-dependent degradation mechanism. Plant Cell **23:** 785–805.

Veljanovski, V., and Batoko, H. (2014). Selective autophagy of non-ubiquitylated targets in plants: looking for cognate receptor/adaptor proteins. Front. Plant Sci. **5:** 308.

Wang, R.-S., Pandey, S., Li, S., Gookin, T.E., Zhao, Z., Albert, R., and Assmann, S.M. (2011). Common and unique elements of the ABA-regulated transcriptome of Arabidopsis guard cells. BMC Genomics **12:** 216.

Winter, D., Vinegar, B., Nahal, H., Ammar, R., Wilson, G.V., and Provart, N.J. (2007). An "Electronic Fluorescent Pictograph" browser for exploring and analyzing large-scale biological data sets. PLoS ONE **2:** e718.

Wu, F.Q., et al. (2009). The magnesium-chelatase H subunit binds abscisic acid and functions in abscisic acid signaling: new evidence in Arabidopsis. Plant Physiol. **150:** 1940–1954.

Yamaguchi-Shinozaki, K., and Shinozaki, K. (2006). Transcriptional regulatory networks in cellular responses and tolerance to dehydration and cold stresses. Annu. Rev. Plant Biol. **57:** 781–803.

Yoshida, T., Fujita, Y., Sayama, H., Kidokoro, S., Maruyama, K., Mizoi, J., Shinozaki, K., and Yamaguchi-Shinozaki, K. (2010). AREB1, AREB2, and ABF3 are master transcription factors that cooperatively regulate ABRE-dependent ABA signaling involved in drought stress tolerance and require ABA for full activation. Plant J. **61:** 672–685.

Zhou, T., Dang, Y., and Zheng, Y.H. (2014). The mitochondrial translocator protein, TSPO, inhibits HIV-1 envelope glycoprotein biosynthesis via the endoplasmic reticulum-associated protein degradation pathway. J. Virol. **88:** 3474–3484.

Zimmermann, P., Hirsch-Hoffmann, M., Hennig, L., and Gruissem, W. (2004). GENEVESTIGATOR. Arabidopsis microarray database and analysis toolbox. Plant Physiol. **136:** 2621–2632.